

83-2744

ENERGY

DOE/PR/06010-T13
(DE83017094)

CONFIDENTIAL

ADVANCED SENSOR DEVELOPMENT PROGRAM
FOR THE PULP AND PAPER INDUSTRY

Annual Report

By
J. R. Whetstone
H. G. Semerjian
C. Presser
A. Gaigalas
J. Potzick

December 13, 1982

Work Performed Under Contract No. AI01-76PR06010

National Bureau of Standards
U. S. Department of Commerce
Washington, D. C.

and

National Engineering Laboratory
Boulder, Colorado



U. S. DEPARTMENT OF ENERGY

DISCLAIMER

This report was prepared as an account of work sponsored by an agency of the United States Government. Neither the United States Government nor any agency thereof, nor any of their employees, makes any warranty, express or implied, or assumes any legal liability or responsibility for the accuracy, completeness, or usefulness of any information, apparatus, product, or process disclosed, or represents that its use would not infringe privately owned rights. Reference herein to any specific commercial product, process, or service by trade name, trademark, manufacturer, or otherwise does not necessarily constitute or imply its endorsement, recommendation, or favoring by the United States Government or any agency thereof. The views and opinions of authors expressed herein do not necessarily state or reflect those of the United States Government or any agency thereof.

This report has been reproduced directly from the best available copy.

Available from the National Technical Information Service, U. S. Department of Commerce, Springfield, Virginia 22161.

Price: Printed Copy A05
Microfiche A01

Codes are used for pricing all publications. The code is determined by the number of pages in the publication. Information pertaining to the pricing codes can be found in the current issues of the following publications, which are generally available in most libraries: *Energy Research Abstracts (ERA)*; *Government Reports Announcements and Index (GRA and I)*; *Scientific and Technical Abstract Reports (STAR)*; and publication NTIS-PR-360 available from NTIS at the above address.

Advanced Sensor Development Program
For the Pulp and Paper Industry

Annual Report
December 13, 1982

REPORT NUMBER 1

National Bureau of Standards
U. S. Department of Commerce
Washington, D.C. 20234

Prepared for the
U.S. Department of Energy
Office of Industrial Programs
Washington, D.C. 20585
Under Contract No. DE-AI-1-76PR06010

TABLE OF CONTENTS

	<u>Page</u>
Table of Contents	i
Executive Summary	ii
1. INTRODUCTION	1
2. TECHNICAL PROGRAM	4
2.1 In-Situ Spectroscopic Flame Temperature Measurement	4
2.1.1 Analytical and Experimental Laboratory Phase	6
2.1.2 Field Experimental Phase	11
2.2 Consistency Measurement	18
2.2.1 Detection Techniques	19
2.2.2 Waveguide Approach	22
2.2.3 Analytical Model	23
2.2.4 Discrete Detection System	27
2.3 Steam Mass Flowmeter Project	28
2.3.1 Operational Description	28
2.3.2 Digital Processing Package	29
2.4 In-Solution Lignin Measurement Research	30
2.5 Evaluation of O ₂ and CO Monitoring Systems for Combustion Controls	31
2.6 Project Summaries	33
2.6.1 In-Situ Spectroscopic Flame Temperature Measurement	33
2.6.2 Consistency Sensor	34
2.6.3 Steam Mass Flowmeter Project	34
2.6.4 In-Solution Lignin Measurement Research	35
3. PLANS FOR NEXT CALENDAR YEAR	36
List of Tables	38
List of Figures	38
References	39
Appendices	40

EXECUTIVE SUMMARY

The National Bureau of Standards is pursuing a basic research and development program sponsored by the Office of Industrial Programs, Department of Energy whose objective is the development of measurement science and technology for on-line measurement of process variables in the pulp and paper industry. Four research projects are currently in progress; (1) in-situ flame temperature measurement, (2) pulp consistency measurement, (3) steam flow measurement, and (4) in-solution lignin measurement.

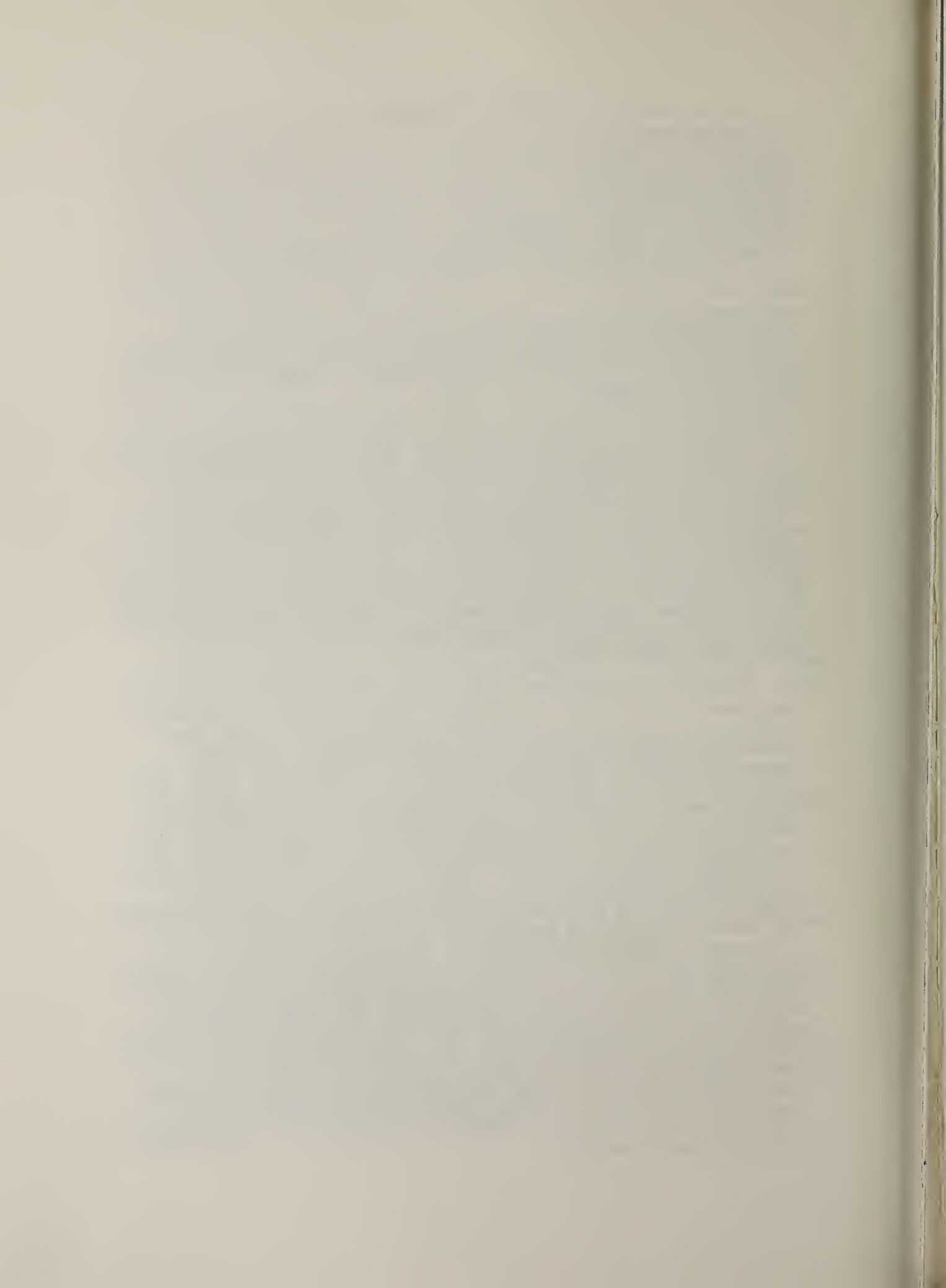
The objective of the in-situ flame temperature measurement project is development of a spectroscopic technique for measurement of flame temperatures and fuel/air mixture ratio in the combustion zone of recovery boilers. The technique utilizes spectral analysis of the emissions of diatomic species formed in the combustion process whose spectral features are located in the ultraviolet and visible regions of the spectrum and are easily distinguished from the intense blackbody radiation emitted by the high concentration of hot particulates in the furnace cavity. These spectral features are very temperature dependent. Both laboratory and field activities are in progress. Models have been developed describing the temperature dependence of these emissions. The models are needed to interpret observations of emissions from laboratory flames and from the recovery boiler. Data from both have been collected. Current activities are directed toward improved field measurement of recovery boiler emissions using high speed optical recording methods, and development of high quality spectral data from combustion of black liquor, both in the recovery boiler and in laboratory combustors. Such data will form the basis for development of the algorithm needed for prototype sensor design and operation.

The objective of the consistency measurement project is the development of a method which is accurate under changing flow conditions, non-intrusive, capable of real-time and on-line measurement, and useful over the range of stock consistency (cellulose concentration) and stream conductivity values found in the pulp and paper mill. A new approach is being taken using radio frequency excitation of circular waveguides. Initial experiments have been completed using a static test cell. These have demonstrated the feasibility of the approach. Current activities are directed toward development of a sensing technique which allows pressurized operation of the sensing section itself. An array of R.F. diode detector/amplifier channels is under development for this purpose. Upon completion this array will be used in a two-inch prototype sensor for sensor response and performance testing on materials of known properties. A two-inch flow loop has been constructed and will be used for tests in paper pulp, and for development of pulp/water mixing rules. The latter is required for determination of consistency values from observed values of dielectric constant and conductivity. Following testing of the two-inch prototype at NBS a six-inch prototype will be constructed for tests at the Institute of Paper Chemistry.

The objective of the steam flowmetering project is development of a new measurement technique of improved accuracy (approximately 1% uncertainty), of greater dynamic range, is non-intrusive to the flow thereby reducing energy loss in metering stations, and measures the average gas temperature. A long wavelength acoustic technique is being developed which is expected to accomplish all of these objectives. A patent application has been filed and non-exclusive licenses have been granted to several private manufacturers. A digital electronic processing package has been designed, fabricated and tested. Initial tests on known air flows at atmospheric pressure have been completed and a paper has been presented at the 1982 Instrument Society of America annual meeting. Currently development of the steam prototype device is underway. Initial laboratory tests in airflows and in steam are planned before the device will be tested in a mill environment.

A new project has been started this year whose objective is the development of a method for measurement of lignin concentration in the liquor solutions found in the pulping process. The need here is a technique which is sensitive to lignin and lignin salts in the presence of the highly conductive and caustic solutions found in the digestion process. A new approach has been conceived which investigates the non-linear coupling of the electric dipole moments of lignin polymers with a radio frequency electric field. The project is in the theoretical and experimental investigation stage to determine the validity of the physical processes involved and the applicability of the technique for on-line measurement of in-solution lignin concentration measurement.

In addition to the four projects underway, one project has been completed. An evaluation of CO and O₂ monitors used for combustion controls has been completed which provides reliable data on their performance, operating range and accuracy. The NBS experimental furnace was used for these experiments. It is equipped with a complete on-line gas analysis system which is used as a reference. Specific areas of interest included evaluation of the accuracy and sensitivity of the measurement techniques over a wide range of operating conditions, correlations of flame stoichiometry with stack measurements, and the effect of stack gas temperature on composition measurements. The O₂ stack gas monitor employed a ZrO₂ type sensor. The system was found to be very sensitive to air leakage when the furnace pressure was kept below atmospheric pressure. A calibration system was also found to be necessary, especially for aspirating type probes. The CO monitoring system is based on infrared absorption across the stack. The CO measurements were found to be quite sensitive to stack gas temperatures. This effect has been quantified in a heated test cell. The relationship between the stack gas CO levels and combustion zone stoichiometry was also found to be sensitive to the energy extraction rate in the furnace cavity. Experimental results have been obtained for both natural gas and No. 2 fuel oil fired systems. A final report has been prepared for publication, and a paper was presented at the 1982 Instrument Society of America annual meeting.



I. INTRODUCTION

The Office of Industrial Programs of the Department of Energy, Advanced Concentration and Evaporation Branch, has supported a basic research and development program at the National Bureau of Standards Center for Chemical Engineering, since July, 1980. The objective of this program has been the development of new measurement science and technologies which will ultimately be applicable to on-line measurement of unit process variables in the pulp and papermaking industry. The measurement techniques developed are such that they will find additional application in measurement and control of unit processes of other industries, as well as in the manufacture of pulp and paper. This program utilizes the advice and assistance of a working group composed of members of the various sectors of the pulp and paper industry, i.e., academia, instrumentation and control system manufacturers, and pulp and paper manufacturers. This group assisted in development of a priority list of process variables for which on-line measurement is currently either fraught with severe systematic errors or is not possible. The list is given in Table I. To broaden the perspective this list provides, a survey was made of the industry by NBS scientists and a report written [1]. The conclusions of this report, which are in agreement with others of a more general nature [2], are:

1. The industry penetration by automatic control systems is high at the paper machine end of the process. This is due to the availability of viable measurement techniques, i.e., sensors which give real-time or nearly real-time process variable information for use by automatic control systems.
2. The pulping end of the process is, by contrast, much less automated by virtue of the lack of reliable on-line process variable measurement technologies (sensors).
3. Specific process variable measurement needs were identified in the pulping end of the cycle. The unit processes of most interest were the digestion process and the chemical recovery cycle, the recovery boiler particularly.

This information and these recommendations have been used to formulate the research program described here. Four research projects are underway and are directed toward developing new measurement technologies for observation of process variables associated with the manufacture of paper pulp or with the preparation of the pulp as it approaches the paper machine for the making of the paper or board sheet. Specifically, these project objectives are: (1) in-situ measurement of flame temperature and fuel/air mixture ratio in the combustion zone of the recovery boiler; (2) measurement of the consistency of pulp slurries; (3) simultaneous measurement of steam mass flowrate and steam temperature; and (4) measurement of lignin

Table 1

ON-LINE MEASUREMENT NEEDS

- | | |
|--|---|
| ° Kappa number (lignin) | ° Pulp quality (freeness) |
| ° Steam flowmeter | ° Active alkali |
| ° Liquor combustion (UV sensor) | ° Smelt bed parameters |
| ° Liquor characteristics
(defined by TE report) | ° Lime kiln T profile |
| ° Percent solids black liquor | ° Consistency (correlation
moment flowmeter) |
| ° Chip moisture | ° Bulk chip density |

concentration in digestion liquors. An additional project has been completed, having as the objective the evaluation of commercially available CO and O₂ sensors. The final report has been completed [3] and a paper presented at the 1982 ISA meeting [4].

The four research projects are specific to the unit processes found at the pulping end of the papermaking process. Two also have application in the pulp preparation or blending operations that are found between the pulp mill and the paper machine itself. The technical activities of these research projects are discussed in the sections below. Some introductory material is included with each to give a perspective of the work relative to the particular unit process involved.

2. TECHNICAL PROGRAM

2.1 In-situ Spectroscopic Flame Temperature Measurement

The objective of this research project is development of a new approach to combustion zone temperature measurement based upon emissions from the combustion zone of a recovery boiler, which can then be related to the combustion zone stoichiometry. The recovery boiler is one of the most capital and energy intensive installations found in the pulping process. It is a key part of the chemical recovery cycle of the pulp making process and performs two tasks. Its primary task is the reduction of the spent pulping chemical derived from the digestion process, primarily the reduction of sodium sulfate to sodium sulfide. Steam production is the secondary task. In many mills the recovery boiler produces a large fraction of the total steam used for electrical generation and process purposes. The recovery boiler employs a staged combustion process. Figure 1 shows the major elements of one of the two predominant types of boiler. Combustion air is introduced to the furnace cavity at three levels. The fuel, black liquor, is injected into the cavity between the secondary and tertiary air injection levels. Black liquor is the concentrated spent cooking liquor of the pulp digestion process. It is a slurry composed of inorganic salts, lignin compounds leached from the wood during digestion, and water. Currently, the normal firing condition is approximately 65% solids concentration. The lignin compounds provide the fuel value of the black liquor. The inorganic constituents, under the influence of the combustion gases, ultimately form a char which falls to the furnace floor forming a smelt bed in which the bulk of the chemical reduction reactions are thought to occur. The resulting char forms a particulate which pervades the furnace cavity and has sizes ranging from one micron to several millimeters. Formation of the char begins with the black liquor droplets issuing from the injection nozzle. These droplets dry and undergo suspended pyrolysis and combustion in the furnace cavity until they fall to the smelt bed. After combustion the char particles remain at high temperatures and strongly emit blackbody radiation. This radiation is located primarily in the infrared region of the spectrum, although the high energy tail of the Planck distribution function may extend into the visible region. Use of emissions from the combustion products for the determination of the combustion temperature requires an approach which is insensitive to this broad range of blackbody radiation, and is specific to the combustion process.

The approach being taken in this project is to avoid the infrared region of the spectrum where blackbody emissions are most intense. Instead, the emissions of diatomic molecules formed as intermediates in the combustion process will be utilized. These species emit radiation in the ultraviolet and near visible region of the spectrum. The concentration of these species is strongly dependent upon flame

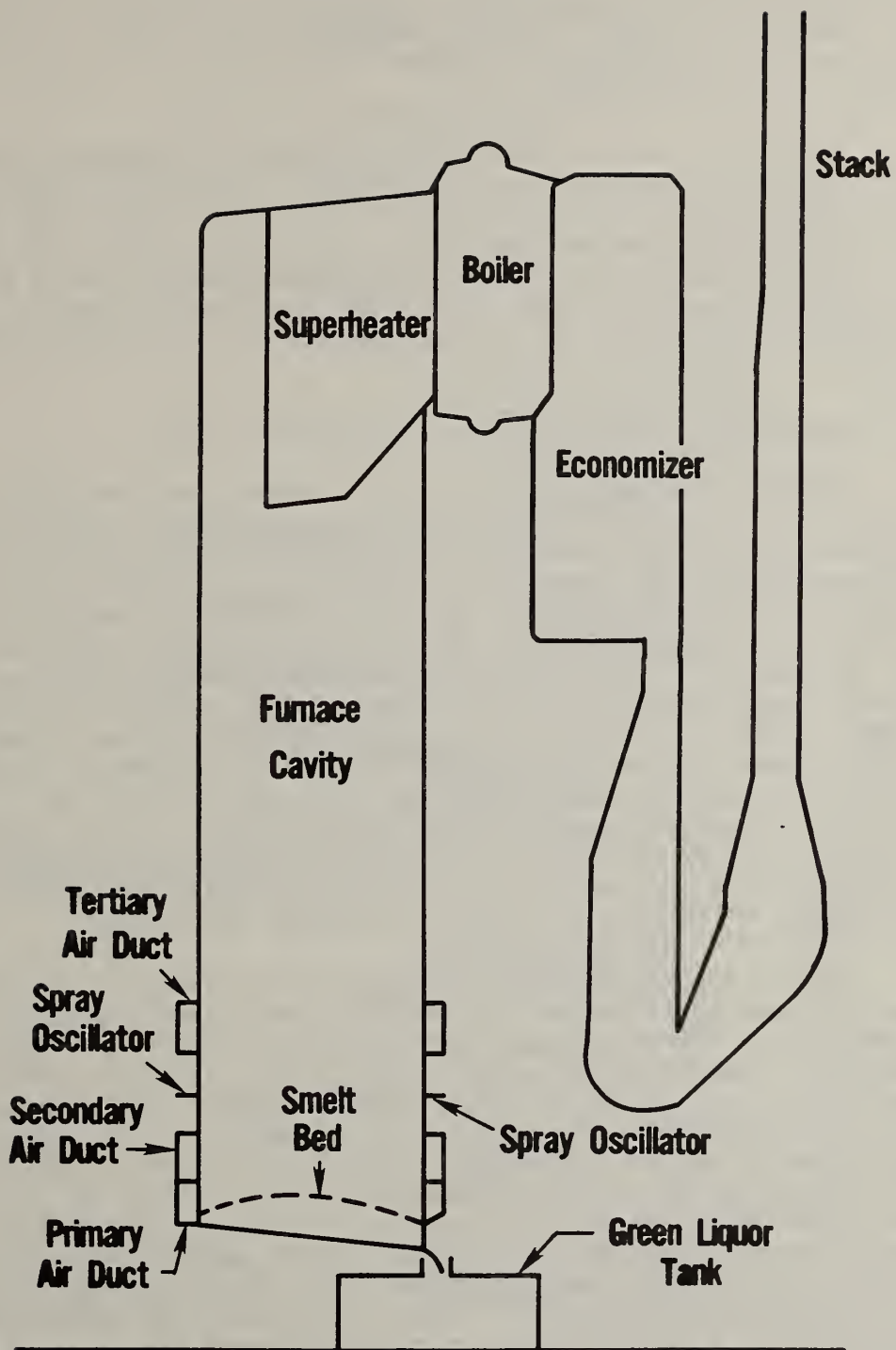


Figure 1. Black Liquor Recovery Boiler

temperature and, therefore, flame stoichiometry. The species of interest include OH, CH and C₂. The research direction of this project is to: (1) quantify the relationships between these emissions and flame stoichiometry; and (2) investigate the effect of continuum emissions from particulates, spatial distribution of emissions, and the effect of burner geometry.

The research effort has taken two parallel directions to date. The first is an analytical and experimental laboratory effort through which a scientific knowledge base is being established. The second effort is a field effort consisting of two phases; the first phase is the gathering of spectroscopic data from operating recovery boilers, and the second phase is testing a prototype device which measures combustion temperatures in various regions of the recovery boiler cavity.

2.1.1 Analytical and Experimental Laboratory Phase

Initial experiments and analytical efforts had the objective of characterizing and quantifying the emissions from OH species formed in methane and fuel oil flames. The experimental part of this work was performed in the NBS experimental furnace and in laboratory flames. Initial spectral measurements were made using a .275 meter spectrometer which has a spectral range of 190 to 600 nm, with a resolution of 0.5 nm. Preliminary experiments were done both in natural gas and oil flames. Spectra were obtained in the 250-500 nm range. In natural gas flames, black body emissions are almost negligible; the OH emissions from the band located at 310 nm ($A^2\Sigma \rightarrow X^2\Pi$ transitions) are very strong; CH emissions both at 390 nm ($B^2\Sigma \rightarrow X^2\Pi$) and 431 nm ($A^2\Delta \rightarrow X^2\Pi$) are also observed very clearly. Both the OH emissions at 310 nm and the CH emissions at 431 nm exhibit strong temperature dependence, and prospects for utilization of these bands for measurement of combustion temperature appear promising.

Similar spectra have been obtained in oil flames. In this case, the continuum contribution from particulates is much stronger and increases in intensity towards the longer wavelengths. These initial experiments were carried out at a single axial location, very near the fuel injection point of the experimental furnace. The preliminary experiments indicated the need for instrumentation with higher spectral resolution to resolve individual lines in the OH and CH spectra. To this end, a 0.5 meter spectrometer was obtained which has a spectral resolution of better than 0.02 nm, with a 1180 line/mm grating. This resolution was demonstrated by resolving the mercury emission doublet at 313.1 nm. Spectra was again obtained in the experimental furnace with both natural gas and oil flames; the quality of the spectra was excellent and a number of very strong lines were identifiable (see Figure 2). These lines were subsequently shown to have strong temperature dependence. The sharp bandhead should also facilitate identification of, and compensation for, blackbody emissions.

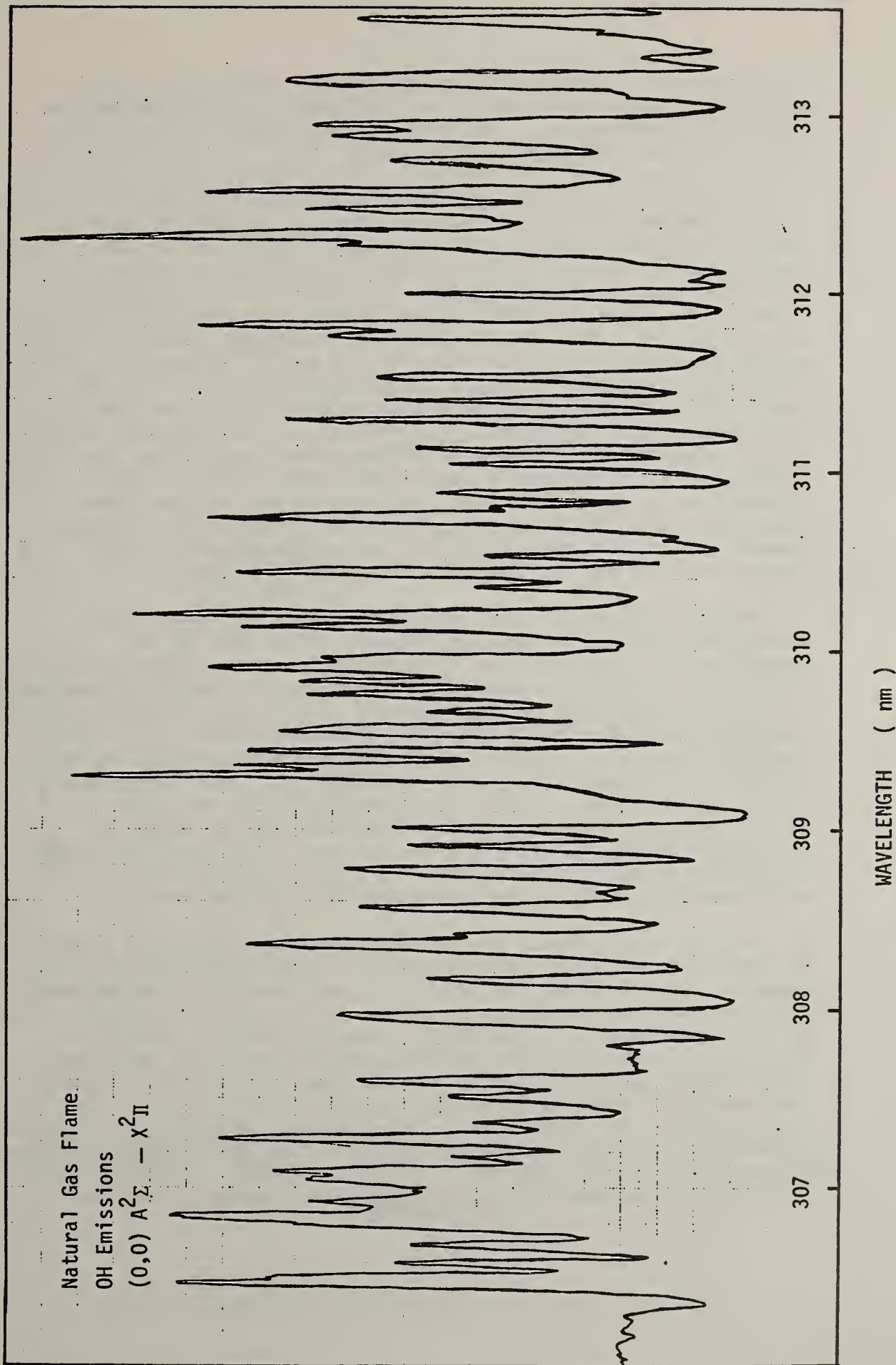


Figure 2. OH Emissions from a Natural Gas Flame

Observation of the emissions confirmed their dependence on the equivalence ratio/stoichiometry of the flames and has provided the initial experimental basis for further investigation of these as a means for flame temperature measurement.

Identification of the spectral lines contained within the observed emission bands is critical since each band is composed of several groups or series of emission lines. Each line and series has a characteristic dependence of emission intensity upon temperature. A literature search was completed of published data on OH emission intensities at various temperatures. These data provide the input for an algorithm developed to calculate the temperature dependence of the emission intensity for lines occurring in the 310 nm band. A computer program was initially developed using this algorithm to compute the temperature dependence for individual emission lines, and some typical results are shown in Figure 3. As the four curves indicate, emission intensity may either increase or decrease for a particular line with temperature. Utilization of appropriate combinations of line intensities is expected to result in an accurate, in-situ flame temperature and combustion zone stoichiometry measurement technique. However, to realize this objective, further development of the laboratory data and the analytical algorithm are needed.

Further analytical developments were directed toward the development of spectral maps or diagrams which simulate the characteristics of the actual spectrometric data. In order to develop a reliable algorithm for temperature measurement, each line observed in a particular band must be unambiguously identifiable in order to know the dependence of emission intensity upon temperature. The initial computer program was expanded to include a plotting capability which results in the spectral map shown in Figure 4. This diagram shows the P1, Q1, and R1 bands of the OH spectrum in the 310 nm region at a single temperature value. A set of diagrams such as these is necessary for each emitting species for each of its emission bands of interest in order to identify the individual emission line intensities and, therefore, obtain temperature information from them.

Models which predict the intensity and the temperature dependence of individual emission lines are useful in identifying each observed spectral line. However, the utility of such models is limited when closely spaced lines overlap in such a way that they cannot be resolved by the spectrometer. In addition, a separate model is needed to predict the spectra of each emitting species. We have, therefore, undertaken an effort to develop a more generalized scheme to predict the spectra of diatomic molecules, including OH, CH and C₂. The model provides the capability to integrate over small spectral regions, simulating a spectral resolution typical of the spectrometer/detector system, using a slit function. The model can also predict emissions from non-uniform temperature and composition fields. A relatively

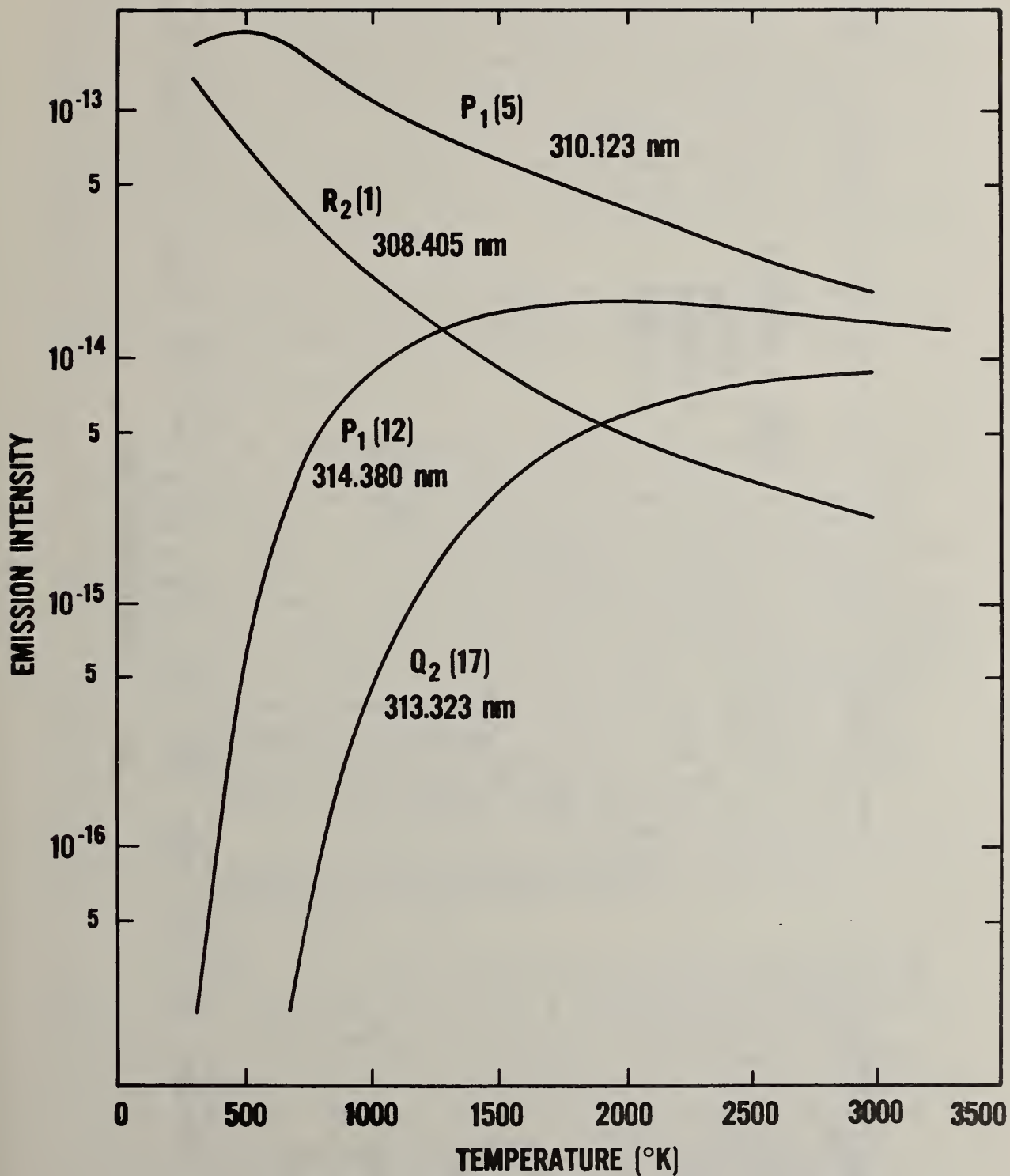


Figure 3. Temperature Dependence of Emission Intensity for the OH P, R, and Q Bonds Near 306 nm

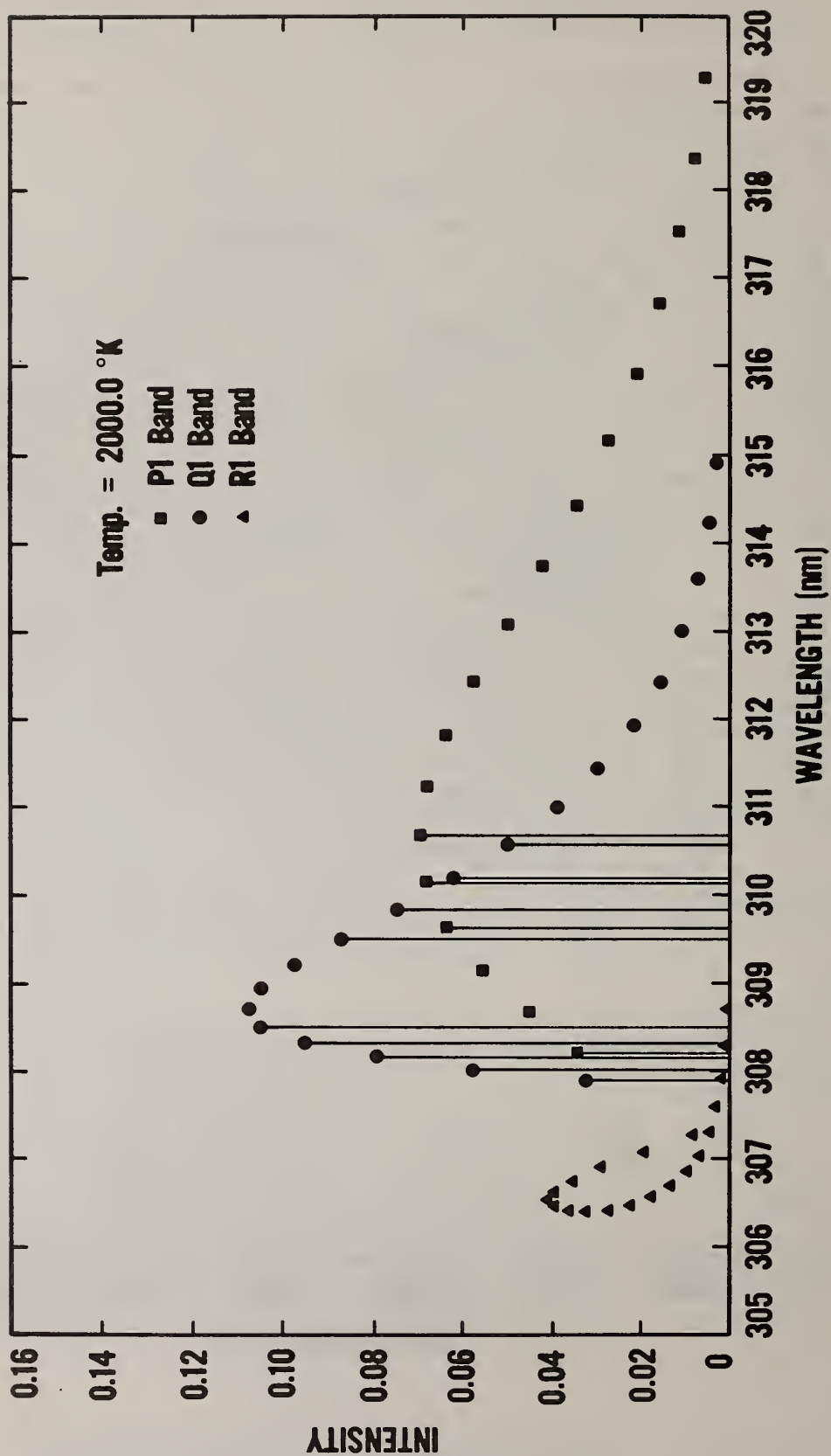


Figure 4. Spectral Diagram - P1, R1, and Q1 Bonds in 306 nm Region

simple model to account for self-absorption is also included. However, line broadening is not taken into account, which would become especially important where self-absorption is appreciable. Present efforts are focused on the extension of the model to include line broadening. Spectroscopic data on CH and C₂ have also been gathered, and the model will be modified to include these species, in addition to OH. An example of typical calculated spectra is presented in Figure 5 for the (0,0) A²_Σ → X²_π transitions of OH at 310 nm for 2000°K. Comparison of Figures 5 and 2 shows the similarity between the observed and predicted spectra. Such spectral diagrams will be utilized in interpretation of the experimental observations, taken with the spectrometric systems being used in this research effort. It will also aid in the selection of the spectral regions that will be utilized for the final sensor configuration.

The combination of spectral models and laboratory experiments in flames will yield the necessary information for quantification of the relationships between emission intensity and flame stoichiometry.

2.1.2 Field Experimental Phase

The parallel field experimental effort has two objectives, (1) to obtain spectral data from operating recovery boilers and (2) to test prototype devices on recovery boilers. Work has begun on the first objective. Such a task differs from that possible in a laboratory environment in three respects; most obvious is the situation of a poor immediate environment. Next it is necessary to develop a method to bring the combustion zone emissions to the spectrometer in such a way that sufficient intensity is available at its entrance slit. Finally, the device must be protected from the rather harsh conditions occurring near the wall penetrations of the recovery boiler. To satisfy these requirements a special optical system was designed and constructed. Its function is to view a particular region in the recovery boiler cavity using one of the boiler's access ports, and to transmit the light gathered from a portion of the combustion zone via an optical fiber to an imaging system mounted at the entrance slit of the spectrometer. This system was built and tested using the NBS experimental furnace. Modifications were made to the initial design to increase the intensity falling upon the entrance slit of the spectrometer.

Subsequently, data was obtained from the recovery boiler of the Westvaco Mill located at Luke, Maryland. These data were not of the quality that are normally obtained in a laboratory environment due to the large and rapid intensity fluctuations of combustion in the recovery boiler cavity. These fluctuations were of such a magnitude and time duration (periods of a few seconds) that only qualitative data could be obtained. The large scale fluctuations were due to the extended time period necessary to record the data taken by the spectrometer. Under normal conditions, i.e., a constant intensity of input light, recording of the spectrometer data is obtained by

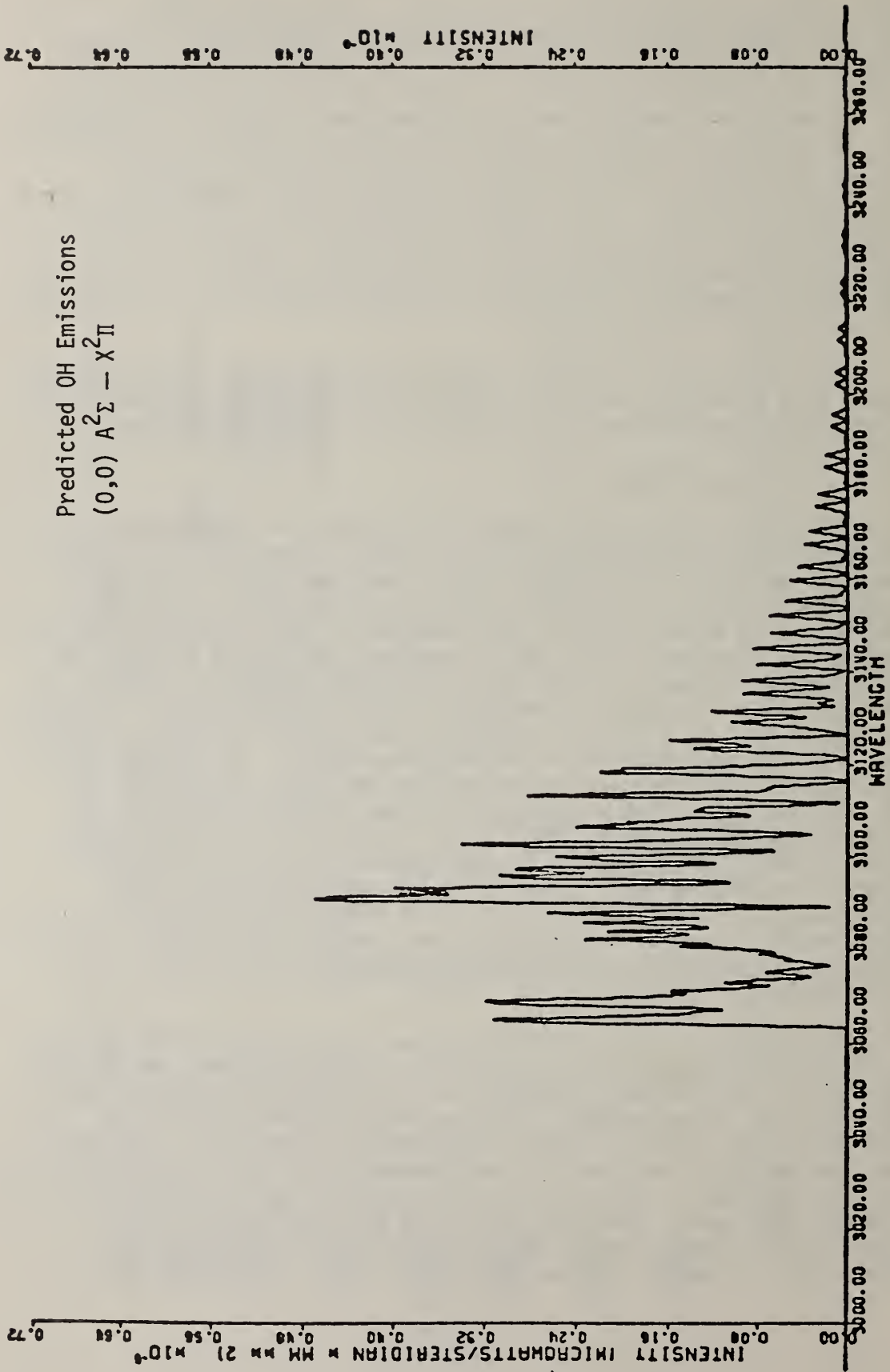


Figure 5. Predicted Emission Spectra for OH in the 306 nm Region for 2000°C

detection of the light intensity passing through the spectrometer's dispersive element and falling on its exit slit behind which a photodetector is placed to measure the intensity of the light passing through the system. The dispersive element is scanned at a constant rate causing the wavelength of the light falling on the exit slit to increase or decrease proportionally with the amount of optical intensity contained in the wavelength region selected by the dispersive element and the entrance and exit slit widths. Recording of the spectral data is accomplished using a strip chart recorder which records the exit slit photodetector output as a function of time. Ten to sixty minutes is necessary to scan a wavelength region of 10 to 100 nm under constant input intensity conditions. As an example, the spectra recorded in Figure 2 required several minutes to record using a constant intensity flame. In order to obtain a useful record of the spectral data the input intensity must remain constant during the recording time. Such conditions can be obtained in laboratory experiments. As mentioned above, the intensity of the visible emissions from the boiler cavity varied considerably over the course of 5 to 10 seconds. These intensity variations carry through to the exit slit of the spectrometer. In all of the observations taken, variations in the input intensity caused such large fluctuations in the spectrometer output intensity that only the presence of gross spectral features could be discerned.

To develop reliable data of the general spectral features from recovery boiler emissions, a data recording technique is necessary which can record the spectrometer output intensity over a wide wavelength range (1 to 25 nm) in a sufficiently short time period (0.10 seconds or better). Recent developments in distributed element optical detector systems form the basis for this new type of readout device and are known as Optical Multichannel Analyzers (OMA). Two of these systems were obtained for evaluation as a detector for the OMA detector which has a sensitive length of approximately one inch with a spatial resolution of approximately .001 inch. Use of the OMA removes the requirement of scanning the dispersive element of the spectrometer. Instead a portion of the spectrum falls on the sensitive region of the OMA's detector, the intensity is digitized and the microprocessor based controller displays the detected spectral region. Such data can be taken quickly; temporal resolutions of 100 nanoseconds are possible. Data collection times of 20 to 100 milliseconds provide good signal-to-noise ratios with the intensities provided by laboratory flames. Typical spectra obtained in a laboratory flame, seeded with black liquor particles, are shown in Figures 6-9. The OMA/spectrometer combination when delivered, will be used for future data acquisition from recovery boilers, and for laboratory experiments needed for quantification of the relationship between flame stoichiometry and emission spectra characteristics.

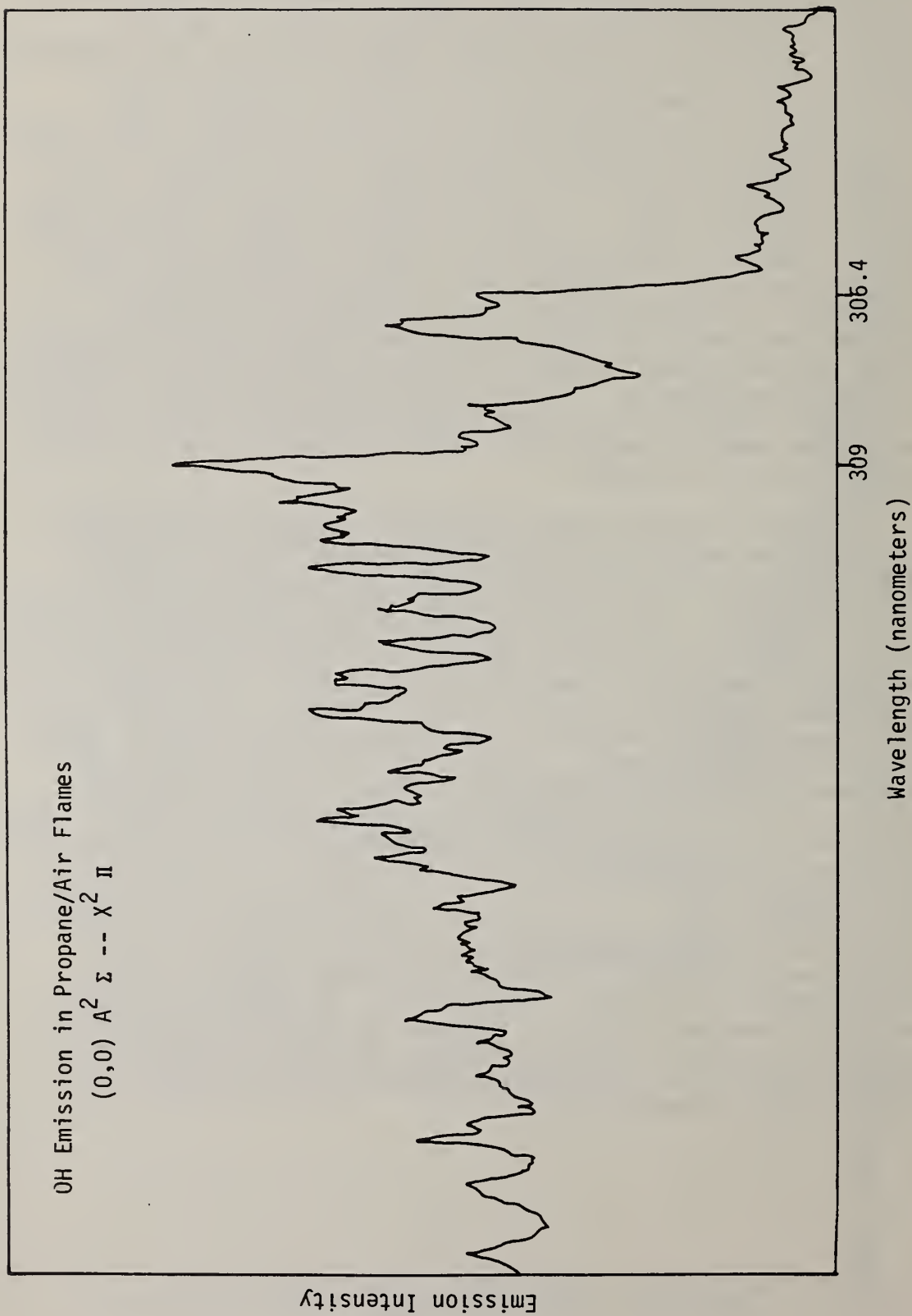


Figure 6. Black Liquor Emissions in the 306 nm Region

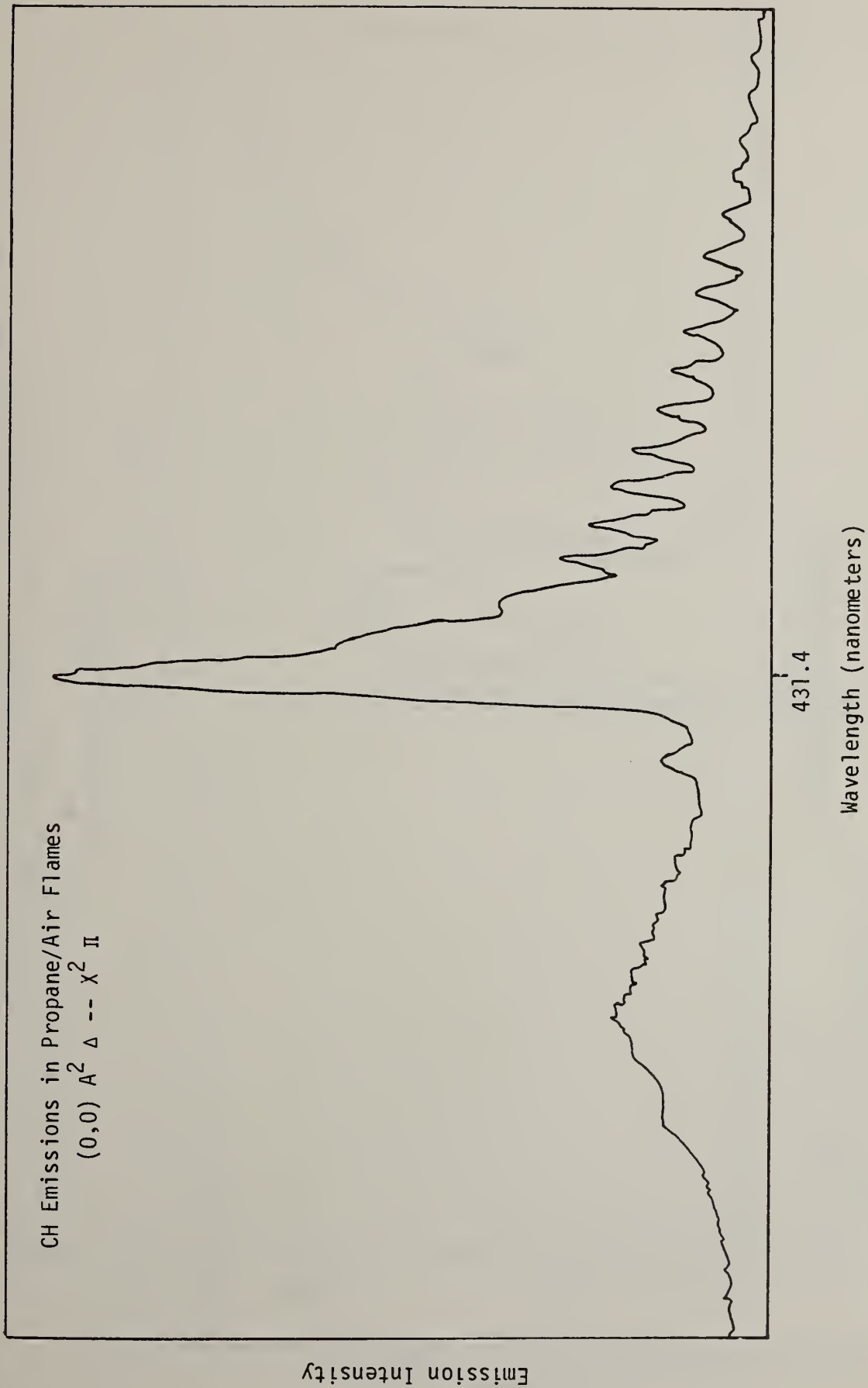


Figure 7. Black Liquor Emissions in the 431 nm Region

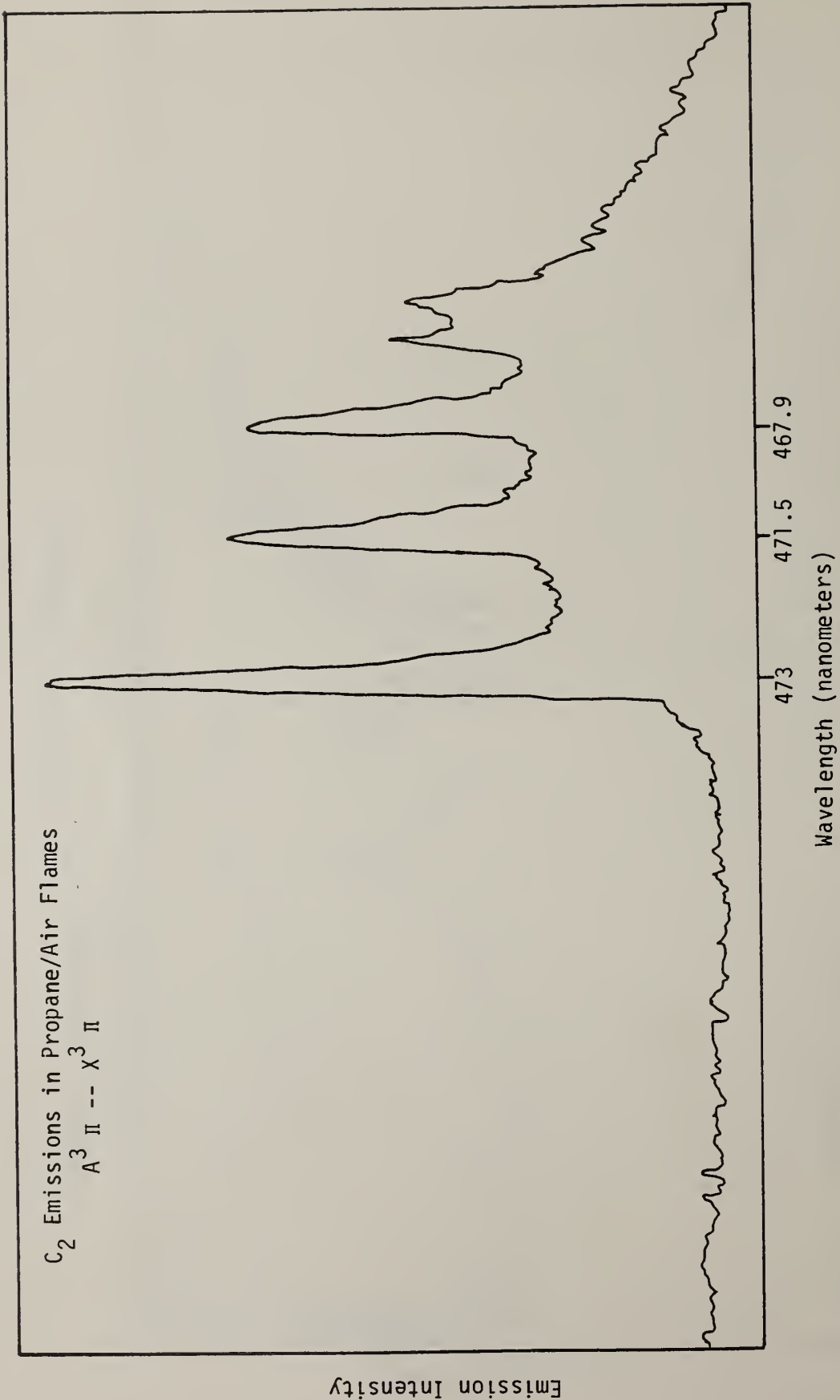


Figure 8. Black Liquor Emissions in the 470 nm Region.

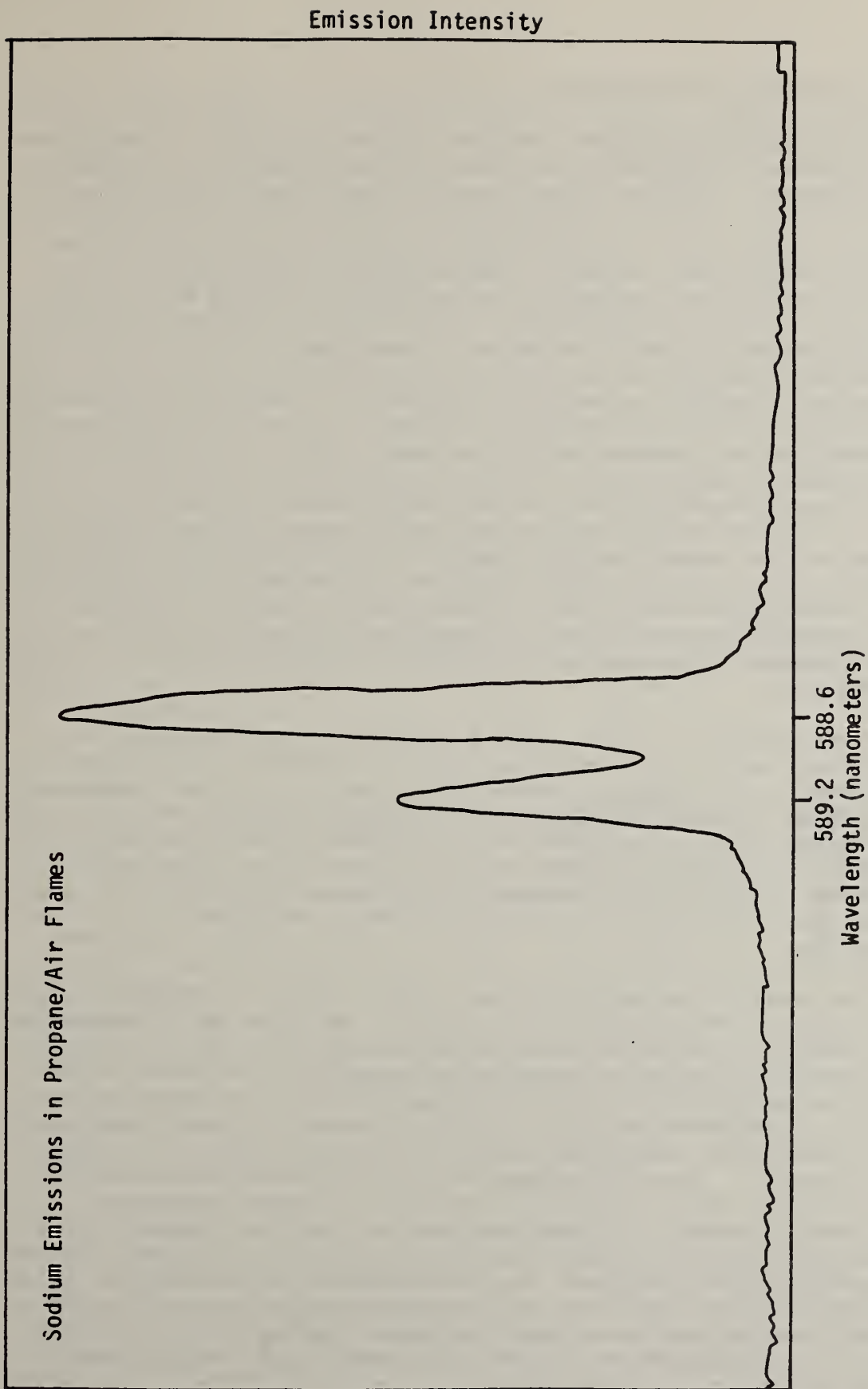


Figure 9. Black Liquor Emissions in the 590 nm Region.

2.2 Consistency Measurement

The papermaking process involves many unit processes in which the process stream is the paper pulp slurry. Pulp slurries are predominately water in which cellulose concentrations range up to 12 to 15 percent to form the solid phase fraction of the slurry. Consistency is the terminology used in the industry to denote solid phase fraction, defined as the mass fraction of dry cellulose in the slurry or paper stock. On-line measurement of consistency in operating mills is largely done using two techniques. The first utilizes the change in reflectance of the pulp with change in consistency. Use of this device in low consistency slurries (up to 2%) slurries is claimed to be effective, sensitive and accurate, especially in the blending processes occurring as the stock is blended with white water to produce stock of the final consistency for use on the paper machine. For higher consistencies however, due to a large decrease in the change in reflectance with change in consistency at higher consistency values, the sensitivity and accuracy of this technique may be considerably degraded. The second technique employs a hydrodynamically shaped body which is immersed in the flow. The contribution to the drag on the body from the cellulose fibers in the slurry is used to infer the consistency value for the pulp. Devices of this type are claimed to be flow dependent, sensitive but inaccurate, and require frequent maintenance.

The objective of this research project is the development of a consistency measurement technique which can be used for real-time measurement, is preferably non-intrusive, not flow property dependent, has a broad range of response, and an accuracy of a few percent in the consistency value. The approach that has been taken is to use the effects of cellulose in stock slurries to modify the propagation characteristics of radio frequency or microwave radiation in circular waveguides relative to the response obtained in water-filled waveguides.

In the past, attempts have been made to measure consistency using the change in the electrical properties of the stock due to changes in the cellulose concentration of the pulp slurry [5]. The electrical property most affected by changing the quantity of cellulose in the stock is the dielectric constant of the mixture. The addition of cellulose (dielectric constant of 2-3) to water (dielectric constant of approximately 80) causes the mixture's dielectric constant to change significantly. Therefore changes in the cellulose concentration in stock slurries may be determined sensitively through measurement of its dielectric constant. A common approach has used low frequency bridge circuits to sense changes in the capacitance value of a parallel plate capacitor filled with stock. In this technique the capacitance is not measured directly but inferred from measurement of the total impedance of the sensing capacitor. Since the total impedance also includes a strong contribution from non-zero resistance values, the conductivity or resistivity of the stock contained between the plates of the sensing capacitor strongly influence the value of the total impedance. Changes

in the total impedance of the sensing element may be the result of either conductivity or dielectric constant changes. Generally, the conductivity is assumed constant, and not measured, either conductivity or dielectric constant changes. Generally, the changes in conductivity are interpreted as dielectric constant, e.g., consistency changes, causing systematic errors in the measurement.

The initial approach of this research project was to use radio frequency techniques to take advantage of the large difference in the values of the dielectric constants of water (approx. 80) and cellulose (approx. 2-3). To reduce or eliminate the effects of changing values of the process stream conductivity the technique preferable should simultaneously measure the conductivity. Given a successful detection scheme for the dielectric constant and conductivity of the stock passing through the sensing volume of the instrument, the development of the appropriate mixing rules for cellulose and water will yield an algorithm for the inference of consistency values from measured dielectric constant values of the stock. This is the approach previously taken by the low frequency bridge technique. The essential difference in our approach is the capability to simultaneously measure the dielectric constant and the conductivity of the stock passing through the sensitive region of the device. Measurement of the conductivity of the process stream is essential since determination of the bulk dielectric constant of the stock is dependent on it at the frequencies of interest.

2.2.1. Detection Techniques

A resonant transmission line technique was chosen for the initial experiments. (This preceded turning of attention to the circular waveguide approach.) A theoretical description of the characteristics of parallel conductor transmission lines was developed which describes the effect of variation in the dielectric and conductivity properties of the medium separating the conductors. The transmission line consists of two parallel wires co-linear with the axis of the pipe carrying the pulp slurry. The circuit shown in Figure 10 was used to measure the response of the transmission line to various excitation frequencies. The detected signals are shown in Figure 11, with distilled water filling the space between the wires. The in-phase signal has a minimum at a frequency f_0 , while the quadrature signal goes through zero at another frequency, f_{90} . For these two conditions the conductivity and dielectric values of the medium separating the conductors can be obtained analytically.

Preliminary data was obtained for distilled water which forms the reference response condition. Also water-methanol mixtures were used to vary the dielectric properties but not the conductivity of the system. Data were also taken on pulp-water mixtures which showed a direct correlation between consistency changes and variation in the frequencies f_0 and f_{90} . These data demonstrated the general

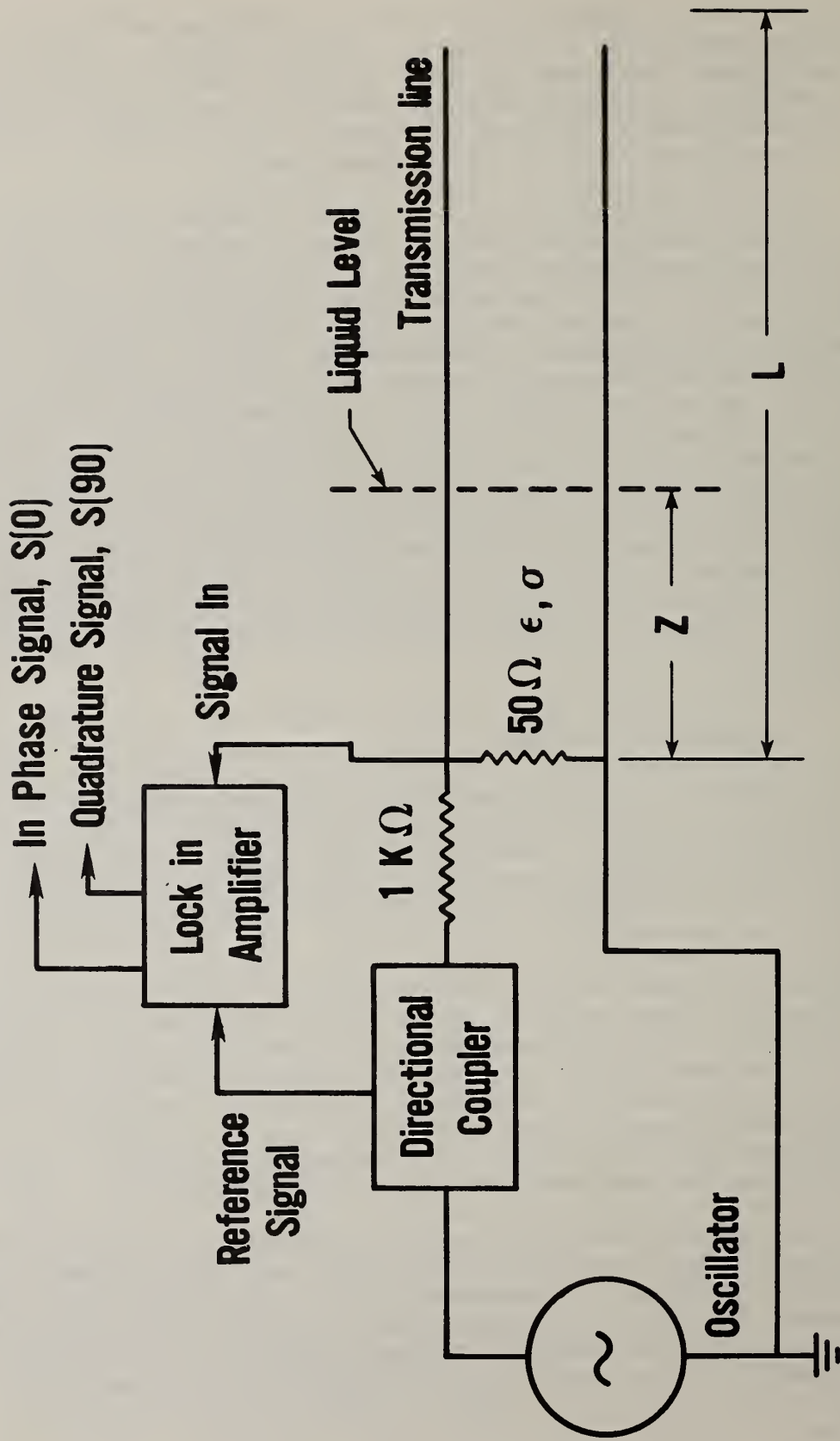


Figure 10. Parallel Conductor Transmission Line Circuit Diagram

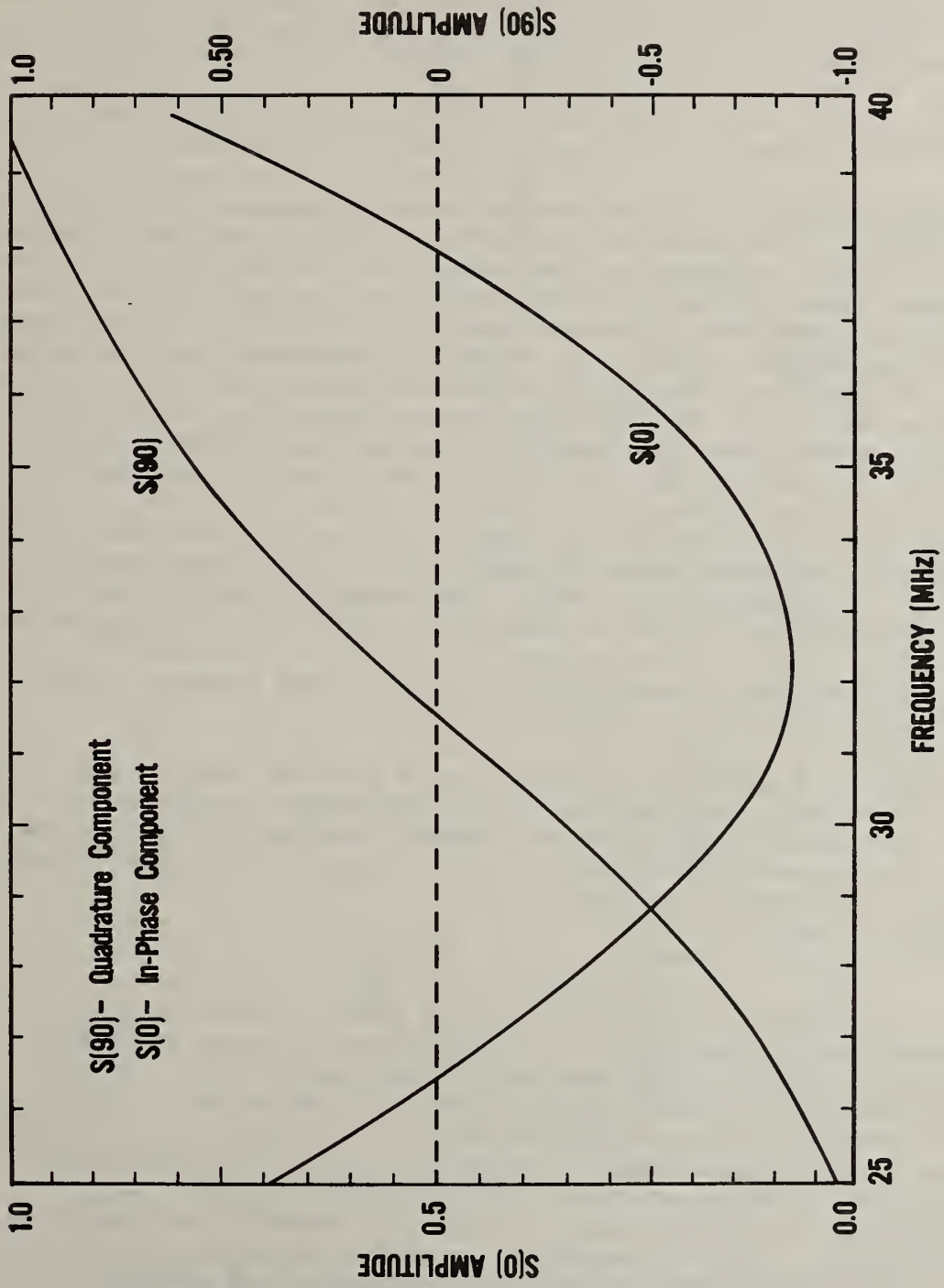


Figure 11. In-Phase and Quadrature Signals - Parallel Transmission Line

validity of the theoretical model of the resonant transmission line system.

The model of the resonant transmission line system describes the interference effects which occur between two electromagnetic waves propagating in opposite directions along the transmission line. One wave travels from the source toward the end of the transmission line. The second wave is produced by the reflection of the initial wave at the end of the line back toward the source. For the interference to be detected, sufficient signal must be reflected to produce a measurable interference effect. A minimum of one wavelength is required.

This initial work used parallel wire transmission lines operating near 40 MHz. This configuration operates well for relatively low conductivities. However, as the conductivity values approach 0.15 mhos/meter the attenuation of the signal is so strong that the strength of the reflected wave is reduced severely, causing interference between the two waves to diminish. The signal is, therefore, reduced below the point of detection. The level of conductivities at which this occurs is comparable to the maximum conductivity encountered in the pulp handling processes of the industry. The maximum concentration of inorganic salts expected to be encountered in process streams is equivalent to approximately 1.2 parts per thousand of sodium sulfate in water [6]. The conductivity of such a mixture is approximately 0.15 mhos/meter, the upper bound of conductivity at which the parallel conductor configuration is useful. Two factors primarily contribute to the undesirability of this approach for pulp consistency measurement:

- (1) The attenuation of electromagnetic waves increases with increasing conductivity.
- (2) The wavelength at 40 MHz is such that the interference pattern extends over distances of 25 centimeters or more which enhances attenuation of the electromagnetic field, thereby decreasing the intensity of the interference signal beyond the limits of detection.

2.2.2. Waveguide Approach

To overcome the limits encountered with the parallel conductor transmission line approach it was necessary to operate at higher frequencies, reducing the effects of ionic conductivity. The attenuation of the electromagnetic field is proportional to the ratio of the conductivity, s , to the frequency, f . In addition, at higher frequencies the wavelength is shorter and the interference pattern occurs over a smaller distance, further minimizing the effects of attenuation. To realize these benefits the frequency must be increased significantly. Use of frequencies above 100 megahertz reduces the effects of attenuation, and the use of circular waveguides for propagation of the electromagnetic field provides a non-intrusive means

of measurement. Circular waveguides, of course, lend themselves very well to process piping. As an indication of the operating frequency ranges available with this approach the cutoff frequencies for pipes of one- and two-inch diameter (water filled) are listed below:

<u>Pipe Diameter</u>	<u>TM(MHz)</u>	<u>TE(MHz)</u>
2.8 cm	710	927
5.0 cm	398	520

The cutoff frequencies are those frequencies below which electromagnetic waves of a given mode cannot propagate in the waveguide. Two modes of propagation are possible for these waveguide geometries, transverse magnetic (TM) and transverse electric (TE). For circular pipe geometries the TM mode propagates at the lowest frequency. By using excitation frequencies below the lowest cutoff frequencies, one ensures that only one excitation frequency propagates and that a simple interference pattern is produced. Experiments were performed in the 2.8 cm (1 inch) diameter pipe at a frequency of 900 MHz and in the 5 cm (2 inch) diameter pipe at 490 MHz. This choice produces the shortest wavelength interference pattern, and at the same time guarantees single frequency operation.

The measurement required to determine values for the dielectric constant and conductivity of the stock filling the pipe, or waveguide, are the wavelength and attenuation of the radio frequency electromagnetic field. Measurements of the axial electromagnetic field strength at the inner surface of the waveguide were made by inserting a small wire through a slit (~ 1 mm wide) cut lengthwise through the pipe wall. The small wire was in turn connected to an r.f. diode mounted on a movable track. Figure 12 shows the voltage output as a function of the location of the detector along the waveguide which is filled with tap water. A strong interference pattern is evident. A theoretical fit was made to the data in Figure 12 assuming that the detector output is proportional to the square of the sum of two waves traveling in opposite directions. The result of the fit is also shown in Figure 12; although there are small discrepancies, the overall agreement between the data and the fit is very good. The results of the fit were used to estimate the wavelength (λ_g) and the attenuation (α). Figure 13 shows the interference pattern obtained with the pipe filled with a 1.3 gram/liter aqueous solution of Na_2SO_4 . This concentration produces a conductivity which is somewhat larger than that encountered in most mill streams. The effect of attenuation is much more evident than in Figure 12. The interference effects are sufficiently large for a measurement of λ_g but with poor results.

2.2.3. Analytical Model

To determine dielectric constant and the conductivity values from the interference pattern measurements, an analytical description or

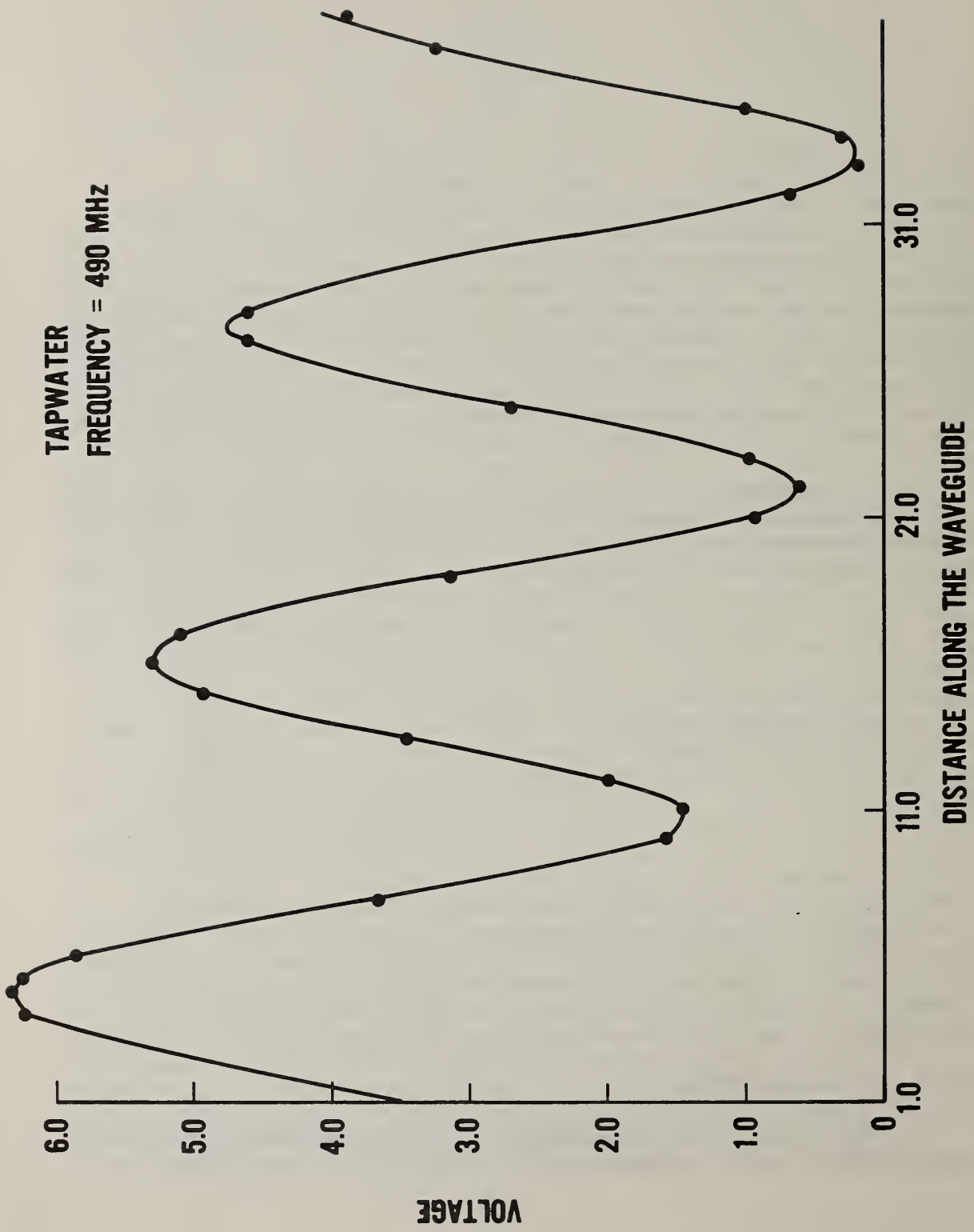


Figure 12. Waveguide Interference Pattern in 2-inch Static Test Cell - Tap Water Filled

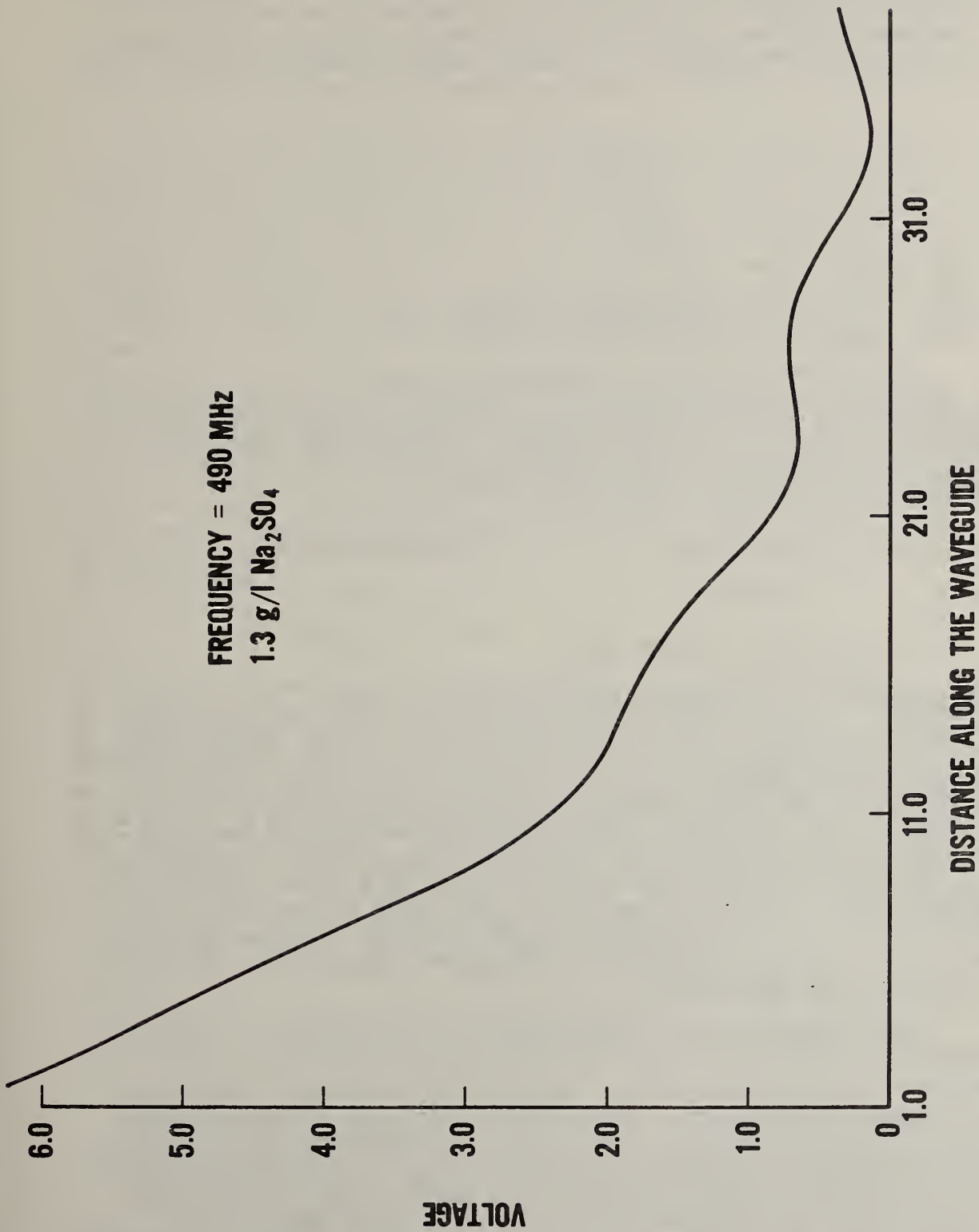


Figure 13. Waveguide Interference Pattern in 2-inch Static Test Cell - Aqueous Solution of 1.3 g/l of Na₂SO₄

model is needed describing the physical phenomena governing the stock-filled, waveguide system. If one assumes that the substance filling the waveguide is homogeneous and its response to the electromagnetic field linear, it is possible to relate the measured quantities, the frequency, f , λ_g and α to the dielectric constant (K) and the conductivity (σ). The relationship is given by

$$K = \frac{10^{11}}{4390 f^2} (\beta^2 - \alpha^2 + (\frac{1.841}{a})^2) \quad (1)$$

$$\sigma = \frac{2533}{f} \beta \alpha, \Omega^{-1} m^{-1} \quad (2)$$

where $\beta = 2\pi/\lambda_g$, f is the frequency in MHz, and a is the pipe radius in cm. Both α and β are in units of cm^{-1} .

To test this theory, measurements were made using a 2-inch I.D. copper tube as the waveguide with an excitation frequency of 490 MHz. Results are shown below. The values of the dielectric constant, K , have been corrected for temperature, and represent the dielectric constant at a reference temperature of 25°C.

<u>Solution</u>	<u>Dielectric Constant</u>
Tap Water	76.69
10% Methanol and Tap Water	73.80

The value of K for tap water should be 78.57 at 25°C. The deviation is most likely due to a small uncertainty in the value of a , the tube radius (5.08 cm was used for calculation). The radius of the waveguide was not highly uniform. An uncertainty or error in the value of the diameter of 0.6% (.012 inches) used in the computation of K would account for the difference between the measured value of the dielectric constant for tap water and the correct value of 78.57. The tube used for the waveguide was egg-shaped by at least this amount. For the methanol-water mixture the decrease in the value of the dielectric constant reflects the decrease in K due to the displacement of polar water molecules by the non-polar methanol much as cellulose fibers would do in the paper stock.

These experiments have demonstrated the feasibility of this approach in detecting changes in the dielectric properties of the medium filling the pipe for low conductivity solutions. Additional experiments were conducted using aqueous solutions of sodium sulfate with a concentration of 1.3 grams/liter to investigate the performance of the technique at high conductivities. Again, the strength of the interference pattern was reduced to the point of non-detectability. These measurements were performed with the radio frequency field injected into the waveguide a small distance from the detection slot of

a static test cell. Reflection of the field from the test cell ends served to generate the counter traveling wave which interfered with the wave emitted by the transmitter. With a more highly conductive fluid in the waveguide the field strength of the initial and the reflected waves were more rapidly reduced causing the interference pattern amplitude in the detection region to decrease.

To increase the strength of the interference pattern a second transmitting station was placed opposite the first with the detection region located in-between. This configuration gives two oppositely directed electromagnetic fields of high intensity traveling through the detection volume of the waveguide. The resulting interference pattern developed between the two counter-traveling initial waves produce an easily detected pattern with a good signal to noise ratio using aqueous solutions of sodium sulfate exceeding concentrations of 1.3 grams/liter. These measurements have demonstrated the feasibility of the approach of simultaneous measurement of conductivity and bulk dielectric constant of the material filling the waveguide. However, questions concerning the sensitivity and accuracy of the technique when applied to paper stock remain. Some measurements were made with a pulp slurry but gave poor results due to flocculation and inhomogeneities of the pulp in the static test cell. These effects are expected to be overcome by flowing stock through the detection region to eliminate flocculation and stratification, and to time average inhomogeneities on the stock flow.

2.2.4. Discrete Detection System

To achieve operation in a pressurized, flowing environment, a system is required for detection of the electromagnetic field strength at the waveguide wall at enough positions to allow reconstruction of the interference pattern with sufficient fidelity to determine the wavelength, λ_g , and the attenuation, α . This requirement must be met in a way which maintains the pressure integrity of the piping in which the sensor is installed. The approach taken is to use a set of 31 equally-spaced holes through which wires insulated from the waveguide pipe wall pass. The tips of the wires are flush with the wall. A RF diode is used as a non-linear detector at each location. The detected signals are filtered, amplified, and multiplexed to an analog-to-digital converter interfaced to a microprocessor. The microprocessor stores the data for several digitization periods and processes it to obtain values for the dielectric constant and the conductivity of the material in the waveguide using the model discussed above.

Development of this approach has begun. The initial detector electronic components have been designed, constructed, and tested, and are operational from the detection diodes to the microprocessor. The sensitivities of the individual detection diodes are not identical. Therefore, a normalization technique is under development to determine the relative sensitivities of the diodes.

2.3 Steam Flow Meter Project

Steam is used throughout the pulp and papermaking process, from the digestion of the wood chips to form pulp to the drying of the paper sheet on the paper machine and the generation of electricity. Most fully integrated paper mills have power generating plants comparable in size to those serving small to moderately sized municipalities. For the most part, metering of steam is accomplished with orifice meters which have a dynamic range of approximately 3 to 1 when used with a single range pressure transducer. The accuracy of this metering technique is dependent upon the condition of the orifice plate itself and the performance of the pressure transducer. The accuracy of determination of the volumetric flowrate is 1 to 5%. The accuracy of the mass flow is dependent upon temperature and total pressure measurement capabilities.

The objective of this project is development of a measurement technique for gases, to be applied to steam, of improved accuracy (approximately 1%) in the mass flowrate with a dynamic range of at least 10 to 1. The approach taken uses a long wavelength acoustic technique which simultaneously measures the volumetric flowrate and the gas temperature. These values combined with geometric dimensions of the meter tube assembly and the total pressure of the gas (steam) give the mass flowrate. This measurement technique is new. It is physically non-intrusive to the flow and is applicable to gases of all types and theoretically applicable to liquid flows, although no experimental work has been done on this application of the technique. The application of the technique to steam flows represents one of the most difficult applications from the point of view of hardness of the acoustic devices (microphones and sound sources) used.

2.3.1 Operational Description

This approach to the measurement of the volume or mass flowrate of a fluid utilizes long wavelength acoustic waves. The frequency is far below the cutoff frequency for the pipe diameter used, therefore the wave propagation along the axis of the pipe is essentially that of a plane wave. As with the consistency measurement approach, two oppositely directed waves are used. The experimental arrangement consists of a loud speaker, which is the sound source, placed upstream (or downstream) of two microphones which are mounted in the pipewall such that they are flush with the inner wall of the pipe. The microphone farthest from the loud speaker is placed a fixed distance from the end of the pipe which is open to the atmosphere. When the sound waves propagating down the pipe from the loud speaker encounter this open end, a large fraction of the acoustic intensity is reflected back into the pipe. The result is two oppositely directed acoustic waves in the microphone region of the pipe. These form a standing wave. For these conditions it can be shown that if the frequency of

the sound field generated by the loud speaker is adjusted until one-half wavelength of the sound field equals the microphone spacing. The velocity of the two waves and, therefore, the velocity of the gas flowing in the pipe, can be calculated from values of the frequency, microphone separation distance, and the pressure of the flowing gas. The type and molecular weight of the gas must be known also. Calculation of the gas velocity requires a measurement of the difference in the phase of the two acoustic waves. The phase difference is the result of the difference in their respective sound speeds as observed from the pipe wall. The mathematical expression describing the standing wave contains terms of the form $c-v$ (upstream travelling wave) and $c+v$ (downstream traveling wave), where c is the sound speed in the stationary gas and v is the velocity of the gas. This sound velocity difference results in a shift in phase between the two waves. The microphones sense the acoustic field strength and these electrical signals are decoded by the processing electronics to determine phase difference. Solution of this expression under the conditions mentioned above yields a value for the gas velocity, v , dependent upon the difference in phase between the two waves and the properties of the gas. The mass and volume flowrates of the gas can be calculated from the gas velocity. A theoretical model has been developed which shows that for the acoustic conditions existing in the pipe, this measurement technique is independent of the velocity profile of the flowing gas, and that the gas temperature, averaged over the cross-sectional area of the pipe, can be obtained from the measurement of the frequency [7]. A complete description of the technique is given in a paper presented at the 1982 Annual Meeting of the Instrument Society of America [8]. The paper is reproduced here as Appendix A.

2.3.2 Digital Processing Package

This year has seen the development of a digital electronic processing package for the flowmeter. Initial tests of the device which demonstrated the feasibility of the concept were performed using an analog processor. This processor employed several phase-locked loop circuits to maintain the frequencies of the two sine waves fed to the loudspeaker, and to detect the signals from the microphones. These required constant adjustment for proper operation. More importantly tests of the flowmeter against the NBS secondary gas flow standards showed a temperature dependent offset. The source of these errors was shown to be the processor. To overcome this temperature dependent offset, and to obtain a stable processing method for use in continued developments of the technique, a digital processor was designed and has been commissioned. This electronic processor uses a 16 bit microprocessor which has been programmed to control a set of specially designed measurement and control circuits necessary for measurement of the phase shift between the two oppositely directed waves in the flow tube and control of the signal fed to the loudspeaker. The microprocessor only performs those tasks which are necessary to maintain the various feedback loops of the flowmeter and provide the

necessary information to a second microprocessor for calculation of the flowrate and gas temperature. Flow tests using the NBS secondary gas flow standards have shown that the magnitude of the offset in the flowrate values has been reduced but not eliminated. Additional tests and improvements of the system will be performed to reduce the offset to a level below 1%.

Incorporation of this technique into pipelines must be accomplished for the technique to be useful for the great majority of the flows encountered in industrial situations whether these are steam or gas flows. Preliminary experiments have been performed to test several schemes to generate the reflected acoustic wave traveling counter to the flow direction. One technique will be selected and implemented in the coming year.

2.4 In-Solution Lignin Measurement Research

A new area of research was begun in the latter part of this year. The general objective is to measure the concentration of lignin and lignin salts which leach into the caustic solutions used in the kraft digestion process. If such a measurement technology can be developed, a new era of control of the digestion process is possible. The degree of removal of lignin from the wood would provide a direct measure of the progress of the digestion process. Desirable characteristics of such a measurement are that (1) it be sensitive to lignin and lignin-salt polymers, (2) it be minimally affected by the high conductivity solutions used in the digester, and (3) that it be capable of on-line measurement. The third requirement need not be so stringent, as we have learned from industry sources. Measurement of the final lignin concentration, in either the spent digestion liquor or in the cooked pulp immediately after, or as the digester is blown down to the brown stock holding tank, is a useful initial objective. A reliable measurement at this point would allow the adjustment of the charge of white liquor to the next batch of chips placed in the digester. Such a technique is useful for batch digester operation, but not so much for continuous digester operation. The full realization of an on-line measure holds the prospect for automatic control of this critical process of the pulp and paper industry, both for batch and continuous digestion.

The initial concept involves a spectroscopic or frequency dependent technique which would observe a unique property of lignin. In this way, the effects of the digestion liquor may be avoided. The initial concept involves the use of the highly polar nature of the lignin molecule. A technique has been proposed which uses non-linear coupling between the lignin molecule and an applied electric field. This coupling mechanism manifests resonant behavior which allows one to discriminate between the high molecular weight lignin molecules and the much lower molecular weight inorganic salt molecules. (Sodium sulfide and sodium hydroxide form bulk of the cooking liquor.) The difference

in molecular weight changes the frequencies at which the applied electric field couples with the dipole moments of the two types of molecules. Coupling frequencies in the range of 10 to 100 megahertz are expected for the lignin polymers, while those for inorganic salts are much higher. Such a large anticipated spread between the resonant frequencies of the constituents of the liquor is expected to allow the lignin constituent to be detected with a good signal-to-noise ratio. Initial tests have shown that the non-linear coupling mechanism exists and is observable in small molecules.

This project is still very much in the exploratory research stage. During the coming year, it is expected to progress to the level of a feasibility testing phase.

2.5. Evaluation of O₂ and CO Monitoring Systems for Combustion Controls

Industrial efforts to improve the efficiency of boilers and furnaces have led to the development of a number of automatic control systems, which regulate the fuel and air flow rates and try to optimize the combustion and energy transfer processes. Most of the combustion control systems rely on measurement of the composition of flue gases, which is then used to adjust the fuel/air mixture in the combustion zone. In the past, gases have been sampled out of the exhaust stream, either in a continuous manner or in batches, and analyzed for a number of species. More recently, in-situ gas analyzers have been developed to provide a continuous reading of species concentration in the flue gases with a faster response as compared to gas sampling systems. The general goal is to keep the fuel/air mixture as close to the stoichiometric mixture as possible, where the combustion and energy transfer processes are optimized, without generating excessive amounts of gaseous and particulate emissions.

The approach generally used for combustion control is to monitor the level of carbon monoxide (CO) and/or excess oxygen in the flue gases, which are used as an indication of deviation from stoichiometric conditions. Optimum combustion performance is usually obtained with slightly fuel-lean flames, due to non-uniform fuel/air mixing. The CO analyzers are based on the measurement of infrared absorption across the stack gases. The concentration of excess O₂ is determined by the electrochemical reaction occurring across a test-tube shaped ceramic probe, made up of yttria stabilized zirconium oxide (ZrO₂). The current practice is to locate these monitoring systems in the boiler stack, far downstream of the combustion zone, where the gas temperatures are low and chemical reactions are assumed to have been frozen or completed. At this point the wall and gas temperatures are low enough, so that any interference due to wall or gas radiation is not expected, and the lifetime of the instruments is substantially increased.

The objective of this study was to provide data on the accuracy and sensitivity of the two measurement techniques over a wide range of operating parameters, and the effect of heat transfer processes on the relationship between the combustion zone properties and stack gas measurements. Performance of the two stack gas monitoring systems, a ZrO_2 type O_2 sensor and an in-situ CO monitor based on infrared absorption, has been evaluated in the NBS experimental furnace. These instruments are typical of in-situ flue gas analyzers that are used for combustion control in boilers and furnaces.

The experiments were designed to compare the measurements obtained with the in-situ CO and O_2 analyzers to those obtained with the gas sampling system and to theoretical equilibrium calculations. Furnace conditions varied from a hot highly radiating environment representative of industrial furnaces, to a cooler environment representative of industrial boilers. Data were recorded over the range of equivalence ratios 0.75 to 1.05 for both natural gas and No. 2 fuel oil. Interest was centered around the desired region for automatic controls; viz., $100 < CO < 300$ ppm, $0 < O_2 < 2\%$ (excess) and $0.95 < \phi < 1.0$.

The ZrO_2 type O_2 monitor performed reliably over a long period of time, and provided quite repeatable measurements with an accuracy of 0.25% O_2 over the full range and a sensitivity of about 2% O_2 per 0.1 equivalence ratio. The instrument, however, did not have a provision for on-line calibration, and the O_2 measurements were found to be quite sensitive to the air aspiration rate, which controlled the gas sampling rate from the stack. The ZrO_2 sensor provides the capability for operating at high temperatures, nominally 2800°F and below, which is valuable especially for high temperature furnace applications. It also means that this sensor could be located closer to the combustion zone, and provide better time response.

Measurements with the in-situ CO monitoring system could only be carried out where the gas temperatures were more moderate, in the order of 700°F. In general, the readings obtained with the in-situ CO monitor were less than half of those obtained with the gas sampling system. This deviation was attributed primarily to the effect of gas temperature on the CO absorption coefficient. This effect was quantified in a set of experiments carried out in a heated cell. These findings indicated that any accurate measurement of CO concentration in the stack gases, using infrared absorption, will require a simultaneous measurement of gas temperature and compensation of the CO measurements. Additional effects due to CO_2 absorption may also be important.

Gas composition measurements obtained in the stack, as the furnace heated up over a long period of time, also displayed a definite effect of furnace temperature and heat transfer processes on the stack gas composition. These results indicate that, for identical

combustion zone parameters, different O_2 and CO measurements could be obtained in the stack; hence, the relationship between combustion fuel/air mixture and stack gas composition is not unique. It can be concluded that the application of stack monitoring systems for combustion control will require a careful study of the characteristics of the particular installation, before a control system can be implemented which will provide reliable control over the narrow range of operation desired for efficient combustion.

These observations also point towards the need for combustion control systems, which do not necessarily rely on stack gas measurements, but rather on measurements made directly in the combustion zone.

Results of this study have been presented at the 1982 Annual Meeting of the Instrument Society of America [3], and a copy of this paper has been attached in Appendix B. A more detailed report has also been prepared on this work, which is in its final stage of preparation and will be published shortly [4].

2.6 Project Summaries

2.6.1 In-Situ Spectroscopic Flame Temperature Measurement

A basic research project is in progress with the objective of developing an in-situ flame temperature measurement technique, which could also be utilized for the control of fuel/air mixture ratio in a combustion system. The approach is based on analysis of spectral characteristics of emitted radiation in the visible and ultraviolet regions of the spectrum. These regions are selected to minimize the contribution of blackbody radiation which is especially intense in the recovery boiler. This project has a laboratory/analytical phase and a field testing phase. In the field experiments data are being obtained on the spectral features of radiation emitted from operating recovery boilers. Future experiments are planned on the spectral features of radiation emitted from operating recovery boilers. Future observations are planned to utilize high speed optical recording techniques. The laboratory/analytical phase of the project consists of analytical work, which is developing information on the temperature response of emission bands of the diatomic species OH, C_2 , and CH, which are formed in the combustion process itself. A model has been developed which generates spectral diagrams of emission bands for temperatures of interest. These are essential in analyzing the data obtained in both laboratory and field experiments. Laboratory data has been developed on OH and CH emission spectra from natural gas and oil flames, also data has been obtained from laboratory burners in which pulverized black liquor particles have been burned. Spectra have been taken from 300 to 600 nm in these flames. These efforts are the initial phase of the study necessary to accumulate a sufficiently broad knowledge base for development of an in-situ flame temperature measurement and combustion control technique.

2.6.2 Consistency Measurement

A basic research effort is underway with the objective of on-line measurement of paper pulp consistency. The technique is electromagnetic in nature and is minimally affected by changes in process stream flow conditions, i.e., velocity profiles, velocity, or swirl number. Two approaches have been attempted. Initial activities focused upon twin conductor transmission lines. This method provided initial insights into the technique but was severely limited by attenuation of the detected signal which was reduced below the threshold of detection by the conductivity of the slurry occupying the space between the two conductors. Successful operation was not possible at the levels of conductivity normally encountered in process streams in the industry. To deal with this problem another approach was taken which uses circular waveguides. In this case, the interference pattern of oppositely directed radio frequency waves is observed. Both the conductivity and the dielectric constant of the medium filling the waveguide can be calculated from these observations. High conductivity values are attainable through the use of dual transmitting points in the waveguide. A prototype device is under development for use in pressurized piping systems. Current efforts are directed toward development of a technique for diode response normalization needed to correctly reconstruct interference pattern characteristics. Once these response characteristics are characterized, the mixing rules for various pulps will be developed using a small flow loop (2-inch diameter, approximately 10 gallons of volume). This loop will be used for extensive testing of the 2-inch prototype and the development of cellulose-water mixing rules. To demonstrate the capability to scale the device up to sizes similar to those normally used in an operating pulp and paper mill a six-inch prototype is planned. It will be tested at the Institute of Paper Chemistry.

2.6.3 Steam Mass Flowmeter Project

A new approach to the metering of gases is being developed which employs a longwave acoustic technique. This technique allows the flow of any gas, such as steam, to be measured using a non-intrusive method which simultaneously measures the mass or volume flowrate and the average gas temperature. Measurement of these parameters allows one to calculate the flow of energy in a steam delivery system. The concept of this unique measurement has been shown to be sound. A new digital processing technique has been developed and tested. Flow tests of the flowmeter against the NBS secondary flow standards on room temperature air flows have shown it to be very linear in its response, but to have a systematic offset which is temperature dependent. The digital processor has eliminated a portion of the offset. Continued developments will be made for closed pipe configuration of the meter and for steam testing.

2.6.4 In-Solution Lignin Measurement Research

A new project has been started this year whose objective is the development of a method for measurement of lignin concentration in the liquor solutions found in the pulping process. The need here is a technique which is sensitive to lignin and lignin salts in the presence of the highly conductive and caustic solutions found in the digestion process. A new approach has been conceived in which the non-linear coupling of the electric dipole moments of lignin polymers with a radio frequency electric field. The project is in the theoretical and experimental investigation stage to determine the validity of the physical processes involved and the applicability of the technique for on-line measurement of in-solution lignin concentration.

3. PLANS FOR NEXT CALENDAR YEAR

The four major projects will continue in the coming year. Two, the consistency measurement and the steam flowmetering project, are expected to reach the field or mill testing stage. At this point, NBS will have completed the research and development work on these measurement technologies. It is hoped that these developments will be utilized by the pulp and paper industry either directly or through purchase from instrumentation suppliers who have developed commercially available products from them. The other two projects will continue in their development. Completion of the in-situ flame temperature measurement technique is expected in calendar year 84. The in-solution lignin concentration measurement project is sufficiently new that the coming year is expected to yield progress in developing the basis for physical understanding of the measurement approach and determination of its ability to detect lignins in aqueous solutions. Specific objectives for each of the projects are listed below.

In-Situ Flame Temperature Measurement -

1. Obtain preliminary data from laboratory flames into which powdered black liquor is injected.
2. Receive the Optical Multichannel Analyzer system and mate it with the 0.5 meter optical spectrometer.
3. Obtain spectra from an operating black liquor recovery boiler.
4. Present a paper at the 14th Annual Symposium on Instrumentation for the Pulp and Paper Industry.
5. Complete laboratory experiments using powdered black liquor particles in gas flames to study the effect of equivalence/temperature ratio on the emission characteristics of black-liquor combustion.
6. Publish an interim report on emission algorithm development and comparison with laboratory and recovery boiler spectral data.
7. Complete conceptual design of prototype sensor.

Steam Flowmeter Project -

1. Complete experiments to determine source of systematic errors in the flowmeter indication and reduce error contribution as much as is feasible. Test two-inch prototype against NBS gas flow standards.
2. Design and construct closed-pipe meter tube, and test against gas flow standards.

2. Rent a package boiler and install at NBS for steam testing of the three-inch prototype of the flowmeter.
3. Construct a three-inch prototype device compatible with mill pressure code requirements and test on air flows against NBS secondary gas flow standards.
4. Conduct mill tests.
5. Publish final report.

Consistency Measurement Project -

1. Complete development of diode response normalization technique.
2. Develop mixing rules for cellulose-water systems.
3. Design and construct six-inch prototype sensor for tests at the Institute of Paper Chemistry (IPC).
4. Complete tests at IPC.
5. Prepare final report.

In-Solution Lignin Measurement Research -

1. Complete design of linear-component test cell and perform tests using known organic solutions.
2. Obtain samples of lignins and perform experiments to determine the sensitivity of the measurement technique.
3. Extend model of the physical mechanism observed.
4. Prepare interim report on the physical model and experimental results.

List of Tables

1. On-line Measurement Needs

List of Figures

1. Black Liquor Recovery Boiler
2. OH Emissions from a Natural Gas Flame
3. Temperature Dependence of Emission Intensity for the OH, P, R, and Q Bonds Near 306 nm
4. Spectral Diagram - P1, R1, and Q1 Bonds in 306 nm Region
5. Predicted Emission Spectra for OH in the 306 nm Region for 2000°C
6. Black Liquor Emissions in the 306 nm Region
7. Black Liquor Emissions in the 431 nm Region
8. Black Liquor Emissions in the 470 nm Region
9. Black Liquor Emissions in the 590 nm Region
10. Parallel Conductor Transmission Line Circuit Diagram
11. In-Phase and Quadrature Signals - Parallel Transmission Line
12. Waveguide Interference Pattern in 2-inch Static Test Cell - Tap Water-Filled
13. Waveguide Interference Pattern in 2-inch Static Test Cell - Aqueous Solution of 1.3 g/l of N_2SO_4

References

- [1] Whetstone, J.R., and Johnsen, E.G., "Sensors for Efficient Energy Utilization in the Paper Industry," to be published as an NBSIR.
- [2] Fam, S.S., "Impact on Energy Conservation of Automatic Control Systems Utilization in the U.S. Pulp and Paper Industry," Thermo-electron Report #TE4265-20.
- [3] Presser, C., Semerjian, H.G., and Juberts, M., "Evaluation of O₂ and CO Monitoring Systems for Combustion Controls," ISA Proceedings, October 18-21, 1982, Vol. 37, Part 3.
- [4] Presser, C., Semerjian, H.G., and Juberts, M., to be published.
- [5] Bently, R.G., and Tasman, J.E., "Consistency Measurement, 1. The Dielectric Behavior of Pulp Suspensions," Report of the Pulp and Paper Research Institute of Canada, PPR/82.
- [6] Private Communication, R. Bareiss, St. Regis, Incorporated.
- [7] Robertson, B., "Effect of Arbitrary Temperature and Flow Profiles on the Speed of Sound in a Pipe," J. Acoust. Soc. Am., Vol. 62, No. 4, October 1977, p. 813.
- [8] Potzick, J.E., and Robertson, B., "Longwave Acoustic Flowmeter", ISA Proceedings, October 18-21, 1982, Vol. 37, Part 1.

ISA PREPRINT

**ADVANCES IN INSTRUMENTATION
Volume 37 Part 1**

LONG-WAVE ACOUSTIC FLOWMETER

**J. E. Potzick
B. Robertson**



Chemical Process Metrology Division

**Proceedings of the
ISA International Conference and Exhibit
Philadelphia, Pennsylvania
October 18-21, 1982**



INSTRUMENT SOCIETY OF AMERICA

67 Alexander Drive

P.O. Box 12277

Research Triangle Park

N.C. 27709

U.S.A.

THE UNIVERSITY OF CHICAGO



LONG-WAVE ACOUSTIC FLOWMETER

J. E. Potzick
B. Robertson
Fluid Engineering Division
National Bureau of Standards
Washington, D.C. 20234

ABSTRACT

An acoustic flowmeter has been developed for measuring the flow of an arbitrary single-phase fluid in a pipe. Sound waves are induced in the fluid at two frequencies, one twice the other. The phases and amplitudes of the waves are detected by two microphones located in the wall of the pipe, one downstream from the other a distance of six diameters or more. The frequencies of the sound are automatically adjusted so that the shorter wavelength is equal to the distance between microphones. The instrument then measures in real time the volume flowrate of, and the sound speed in, the fluid, independent of fluid composition or temperature. If the fluid is a gas and its molecular weight and specific heat ratio are given, the instrument calculates the temperature. Also, given an independent measurement of the pressure in the pipe, the instrument calculates gas density and mass flowrate. The device is nonintrusive, bidirectional, operates in a noisy environment, and responds to rapid changes in flow and temperature. Because the waves are much longer than the pipe diameter, the measurements are independent of the flow, temperature, or density profiles.

INTRODUCTION

Ultrasonic flowmeters⁽¹⁾ are not entirely successful in measuring gas flowrate in a pipe. Those based on a Doppler principle will not work unless there are particles to shift the frequency of the ultrasound. Those measuring the time of flight of a short ultrasound pulse do not work well in flows containing even a moderate level of noise because producing a jitter-free pulse that is loud enough to be reliably detected over the noise is too difficult. Those using a continuous wave are not entirely satisfactory for a more complicated reason. Ultrasound in a pipe consists of many high-order spatial waves. These modes superpose at a microphone to form a sinusoidal function of time whose phase depends on the phases and amplitudes of all the spatial modes. Unavoidable temperature changes in the gas cause these amplitudes and phases to vary in an extremely complicated and uncontrolled way. The result is a shift in the phase of the detected sinusoid that depends on the temperature in an unpredictable way. This phase shift leads to a shift in the flowrate indication that is indistinguishable from that caused by the flow to be measured. On the other hand, ultrasonic flowmeters are available for measuring liquids flowrates in a pipe, but they all give an indication that is flow-profile dependent.

We have developed a long-wave acoustic flowmeter⁽²⁾ that attempts to avoid these problems. In contrast to ultrasonic flowmeters, this instrument uses sound whose wavelength is much longer than the cutoff wavelength of the pipe so that only the fundamental or plane-wave mode propagates⁽³⁾. This eliminates the strong temperature dependence of the flow indication offset that occurs with ultrasonic flowmeters. It also results in measurements that are averages over the cross section of the pipe, independent of any nonuniformity in flow, density, or temperature⁽⁴⁾. No parts of the flowmeter protrude into the fluid being measured, so the device produces minimal pressure drop.

In what follows, a brief description is given of the flowmeter's principle of operation, its physical design, and some preliminary test results. An analog prototype flowmeter is described which, however, displays such deficiencies as a zero offset as large as 8 percent of full scale over a gas temperature range of 100°C, and an offset drift as the circuits warm up. A digital design is then described which should overcome these difficulties, but at this time has not yet been fully tested. A complete mathematical description of the operation of the flowmeter will be presented in another paper⁽⁵⁾.

PRINCIPLE OF OPERATION

A schematic diagram of the acoustic flowmeter is shown in Fig. 1. Two microphones, small compared to the diameter of the tube, are placed at the top of the meter tube and spaced longitudinally six diameters apart from each other. The microphones are mounted in the wall with their diaphragms flush with the inside surface of the tube. A loudspeaker is connected to a branch from the tube at least two diameters upstream or downstream from both microphones. The sound generated by the loudspeaker has a wavelength that is much longer than the diameter of the tube, and so only the fundamental spatial mode or plane-wave mode propagates. Higher order spatial modes decay exponentially with a decay distance that is shorter than 0.275 times the pipe diameter. Thus, at the microphones the sound is a plane wave with the pressure essentially constant across the cross section of the pipe, and the microphones detect that pressure⁽³⁾. The sound undergoes multiple reflections by elbows, tees, valves, and open ends, both upstream and downstream of the microphones and loudspeaker. The reflected acoustic waves combine to form two sine waves at the microphones, one wave travelling upstream and one downstream, with velocities $c-v$ and $c+v$, respectively, where v is the velocity of the fluid and c is the sound speed in the fluid when it is stationary. The amplitudes of these waves will not in general be equal. If the loudspeaker is upstream of the microphones, the downstream wave in the vicinity of the microphones is the superposition of waves direct from the loudspeaker and from all upstream reflectors. It is incident on the downstream reflectors, and the reflected waves superpose to form the upstream wave in the vicinity of the microphones.

The superposition of the upstream and downstream travelling plane waves forms a standing wave whose amplitude does not quite vanish at the nodes (or minima) as shown in Fig. 1. Care must be taken to avoid placing the microphones near nodes where the acoustic amplitude is too small to give an adequate signal-to-noise ratio. This may involve some testing of microphone locations to ensure adequate amplitudes in an existing closed piping system before a suitable location is chosen.

Because the signal detected by each microphone is a superposition of sine functions of the same frequency, it will be sinusoidal in time. The difference in the phases of the sinusoids detected by the two microphones is in general a complicated function of the sound wavelength, the piping geometry, and the average Mach number $M = v/c$. We limit the following discussion to a Mach number less than 0.1. Then if the distance between microphones is an integer multiple of one half the wavelength, the phase difference becomes considerably simpler⁽⁵⁾. The wavelength λ_n will satisfy this condition, $\lambda_n = 2L/n$, when the frequency f_n of the wave satisfies

$$f_n = nc/2L. \quad (1)$$

Here L is the microphone spacing and n is a whole number. Since a long wavelength is desired, n is generally 1 or 2, so the microphones are one-half wavelength or one wavelength apart. When Eq. (1) is satisfied, the phase difference $\Delta\phi_n$ can be shown to be

$$\Delta\phi_n = n\pi M, \quad (2)$$

independent of the relative amplitude of the waves. This phase difference arises because the flowing fluid drags the sound downstream, increasing the sound speed in the downstream direction and decreasing it in the upstream direction. When the flow changes direction, the phase difference changes sign. The relation between phase difference and Mach number turns out to be exact for any Mach number less than 1 and is valid for all single-phase fluids of low acoustic attenuation.

The amplitudes of the sinusoids at each microphone are used to set the operating frequency to achieve the above results as follows. When the distance between microphones is an integer multiple of one half the wavelength, the amplitude at that frequency will be the same at the two microphones. This can be seen in Fig. 1. Thus the ratio of amplitudes at the two microphones will be one. This ratio is unity only at the operating frequency and at other specific frequencies that are far enough away from the operating frequency that no confusion results when using this ratio to determine the operating frequency. The difference between this ratio and unity can be used with integral feedback to control the frequency. The time integral of this difference can be used to control the frequency of an oscillator which generates a frequency equal to the correct operating frequency.

Once the frequency is set, the speed of sound can be determined by measuring the frequency and using the known distance between microphones. The average velocity of the fluid is then the average Mach number times the speed of sound. The total volume flowrate is this velocity times the cross sectional area. These quantities are directly measurable without knowledge of the type of fluid in the pipe, provided the fluid has low sound attenuation. These results are summarized in Fig. 2.

If the fluid is a real gas its equation of state can be written

$$mP = \rho RT, \quad (3)$$

where m is the molecular weight of the gas, P is the absolute pressure in the pipe, ρ is the

gas density, R is the molar gas constant, $Z(P,T)$ is the compressibility factor for the gas⁽⁶⁾, and T is the average temperature of the gas. The compressibility factor Z , which is 1 for an ideal gas, becomes quite significant at pressures and temperatures near the critical point. The relationship between the gas temperature and the sound speed can now be determined⁽⁷⁾, and the temperature, density, and mass flowrate can be calculated from phase and frequency measurements, as shown in Fig. 2, where it has been assumed that $Z = 1$. This assumption leads to a -0.04% error for dry air at 0.05 atm and 33°C, a 0.03% error at 1 atm and 25°C, and a -1.64% error at 40 atm and -3°C⁽⁸⁾.

The total mass flowrate can be obtained by multiplying the total volume flowrate by the gas density. The result is

$$G = \gamma P A \Delta t / L \quad (4)$$

where G is the mass flowrate, γ is the specific heat ratio, P is the absolute pressure, A is the cross-sectional area, $\Delta t = \Delta \phi_n / (2\pi f_n)$ is the time difference between sinewaves, and L is the distance between microphones.

This formula is correct to within 1 percent for air at atmospheric pressure flowing with a Mach number less than 0.1. There will be other sources of error which have not yet been identified or quantified.

The response time of the acoustic flowmeter to changes in flowrate can be on the order of the period of the sound frequency used. In practice, however, many periods usually are averaged to smooth the effects of flow fluctuation and turbulence, but the response may still be considered to be real-time for many applications.

In addition, since the phase measurement is bidirectional, the flow indication is also bidirectional, with no preferred direction. If the flow changes direction, the flowmeter response will pass linearly and smoothly through zero. The uncertainty as a percent of reading may increase, though, at very low flowrates. The magnitude of the zero offset has yet to be measured.

The flowmeter is easily scaled to different pipe diameters. The only requirement is that the microphone spacing must be maintained at least as large as six diameters. For small pipes, the spacing need not be as short as six diameters. For large pipes, the spacing must increase with the pipe diameter. Increasing this spacing decreases the operating frequency. This may require changing the loudspeaker so that it is better matched for the new frequency.

PHYSICAL DESIGN

A prototype acoustic flowmeter has been fabricated for use in air at atmospheric pressure and temperatures from about 0° to more than 100°C. It uses a 5.08 cm diameter brass meter tube about 70 cm long, as shown in Fig. 3. The metal wall of the meter tube must not transmit sound directly to the microphones at the operating frequency. So a rubber vibration isolation coupling is used between the loudspeaker section and the meter tube, and the microphones are mounted elastically as shown in Fig. 3. One way of helping to minimize the generation of

bending modes of the pipe may be to use two loudspeakers mounted symmetrically on opposite sides of the pipe. However, even with this symmetric mount, elbows or tees elsewhere would generate bending modes. Thus other efforts may be necessary to discourage sound propagation in the pipe walls, especially the bending modes, but also modes that distort the pipe cross section. A meter tube of a material with high intrinsic damping, such as polyvinyl chloride or a fiber composite may help.

The microphones used are 1/4-inch quartz dynamic pressure transducers with a resonant frequency of 250 kHz. Wide bandwidth is necessary in order to reduce the phase shifts of the microphones to negligible values⁽⁹⁾. If the sensitivities of the two microphones are not exactly equal, the voltage amplitude ratio used to determine the operating frequency will not equal the acoustic amplitude ratio. As a result the feedback will not set the frequency generated by the loudspeaker equal to the correct operating frequency. To avoid this error, the flowmeter uses two frequencies, one twice the other, at f and $2f$. The correct frequency is obtained only when the amplitude ratio at one frequency equals the ratio at the other, even though these ratios may not equal 1. The difference in these ratios is taken as the frequency error signal, and the time integral of this quantity is the frequency input to the oscillator that generates the required sine waves.

For the 30.5-cm spacing between microphones, the lower frequency is about 560 Hz at room temperature. This frequency is clearly audible, and can be heard to increase as the temperature of the gas increases. This meter may be inappropriate in applications where a low ambient sound level is required.

Phase measurements can be made for either frequency. However, in the following, values at the lower of the two frequencies are stated.

We choose full-scale flowrate to correspond to the Mach number equaling 0.1. The most recent prototype can measure flows nearly five times as fast, but the smaller number gives the range over which the linear formula in Eq. (4) is correct within 1 percent. The sensitivity of the measurement of the velocity v with respect to the measurement of the phase difference $\Delta\phi$ is $\Delta\phi/v = \pi/c$. This is independent of the flowmeter dimensions. The phase difference at full scale is easily seen to be 0.1π or 18 degrees. The full scale value for the time difference Δt is the above divided by $2\pi f$, or $0.1/(2f_1)$, which is 88 microseconds at 25°C. The full scale value for the volume flowrate at 25°C in a 5-cm diameter pipe is 70.2 liters/second. The full scale value for the mass flowrate at atmospheric pressure in a 5-cm diameter pipe is 83 grams/second (g/s). Pertinent data for the prototype flowmeter is summarized in Fig. 2.

If we require 1 percent resolution of a reading of 10 percent of full scale, then we must be able to measure Δt with 88 ns resolution. The acoustic noise that is always present in flowing fluids complicates this task. In addition, the microphones, their amplifiers, and any following electronic circuits must not introduce phase uncertainty which leads to a time delay greater than 88 ns, even as the operating frequency changes. Hence the need for wideband microphones and electronics mentioned earlier.

An early version of the acoustic flowmeter used mostly analog circuits to process the microphone signals. Voltage-controlled phase shifters and synchronous detectors were used in a feedback arrangement to measure the phases and amplitudes of the microphone signals at each frequency⁽¹⁰⁾. The ratio difference used for the frequency error signal was obtained with analog dividers and a differential integrator. The time-integrated frequency error then set a voltage-controlled oscillator to $2f$. This frequency was divided by two, and the two frequencies were shaped into sine waves, added, and amplified to drive the loudspeaker. The time difference Δt was determined from the phase measurements of the microphone signals at frequency f and used with a measurement of the frequency f to calculate the temperature and mass flowrate. A more complete description is given in Ref. (2).

This analog version was tested on the air flow calibration facilities at the National Bureau of Standards (NBS), and the results are shown in Fig. 3. Here the indicated mass flowrate calculated from Eq. (4) using the parameter values for air at atmospheric pressure. The straight line is the result of a least squares fit to the data below full scale, which is Mach 0.1. The slope of this line is within 1 percent of the expected value of 1, but there is an offset of 0.25 g/s, which is about 0.3 percent of full scale. The two data points above Mach 0.1 fall below the line. This is most likely due to a temperature dependence of the offset, since the temperature of the air flow decreased from room temperature at lower frequencies to 0°C at the highest flowrate.

The analog flowmeter has also been tested at temperatures up to 100°C. Over this temperature range, an offset as large as 8 percent of full scale has been observed. In addition, the analog flowmeter had a flow-indication offset which varied in time as the electronic circuitry warmed up.

In order to overcome the latter offset and to make changing design parameters easier, a new digital version of the acoustic flowmeter has been constructed, but not yet tested or debugged. A Fourier coefficient technique is used to measure the amplitudes and phases at the microphones. This technique provides the required resolution in the presence of wide-band and harmonic noise without the use of narrow band filters. The latter could introduce a phase shift that is indistinguishable from the phase shift to be measured.

Processing of the microphone signals is done in three stages in this digital prototype as shown in Fig. 5. The stages in order are a hard-wired parallel processor, a serial processor or microcomputer programmed in assembly language, and a small desktop computer programmed in a high level language. The earlier stages provide greater speed of computation, and the later stages provide easier design and programming with the possibility of changing parameters to fit different conditions.

In the first stage, the parallel processor computes Fourier sine and cosine coefficients at each of two frequencies for each microphone, eight coefficients in all, and sends them to the serial processor at the end of each acoustical period. A block diagram of the parallel processor is shown in Fig. 6. The microphone signals are amplified and digitized with 8 bits resolution, 256 times each acoustical period. These digital signals are then applied to one input of each of four multiplier-accumulators operating in parallel for each microphone. A master clock, whose frequency is set by the serial processor to $256 f$, toggles an

8-bit counter whose output cycles sequentially through 256 addresses each 8 bits long. This output is connected to the address inputs of four read-only memories so that they are addressed simultaneously. These four memories have been programmed with the functions $\sin f$, $\sin 2f$, $\cos f$, and $\cos 2f$, respectively. Since the memories are always enabled, they output these functions in a periodic manner. These data outputs then go to the other inputs of the multiplier-accumulators as shown. Two hundred fifty-six products are then accumulated on each of the multiplier-accumulators during the acoustic period, thus forming the eight Fourier coefficients. This integration provides some of the discrimination against nonsynchronous noise. At the end of the acoustic period, the coefficients are loaded into registers that can be read by the serial processor, and an interrupt is generated. The outputs from the $\sin f$ and $\sin 2f$ memories are also converted to analog form, mixed, and amplified by a 70-watt audio amplifier to drive the loudspeaker.

On interrupt, the microcomputer, which is an AmZ8002 evaluation board, fetches the eight Fourier coefficients. It uses them to calculate the amplitudes of the signals detected by the microphones and adjust the amplitudes of the signals sent to the loudspeaker so that the detected amplitudes remain within the correct range. The gain of the microphone amplifiers can be set to obtain any desired signal-to-noise ratio within the power limitations of the loudspeaker and its power amplifier. The microcomputer then calculates the difference of amplitude ratios to get the frequency error, integrates it, and uses the result to increment or decrement the operating frequency f as necessary. When the amplitude and frequency errors are sufficiently small, the microcomputer uses trigonometric identities and a look-up table to calculate the phase difference between the microphone signals. It averages this phase difference over a user selectable number of terms. This provides further noise discrimination. When the average is complete, the microcomputer sends the frequency f and the average phase difference through a serial port to the desktop computer.

In the third stage, the desktop computer calculates and displays the gas temperature, the volume flowrate, and the mass flowrate in engineering units. This computer can also send new parameters to the microcomputer to change such things as ranges and number of terms in averages.

CONCLUSION

An acoustic flowmeter has been designed which has many advantages over conventional flowmeters. Such a meter has been built with analog circuits and tested and has demonstrated the soundness of the principle, although some deficiencies in the implementation were revealed. A second flowmeter is being constructed with digital circuits. We expect this digital version of the acoustic flowmeter to perform better than the earlier analog version. Testing to quantify its performance is planned.

REFERENCES

1. Lynnworth, L. C., "Ultrasonic flowmeters," published in "Physical Acoustics," Vol. 14 (Academic Press, 1979), pp. 407-525.

2. U.S. Patent Application SN 300,830; foreign patent applications being filed.
3. Morse, Philip M., and Ingard, Uno, "Sound Waves in Ducts and Rooms," Theoretical Acoustics, McGraw-Hill Book Co., New York, N.Y., 1968, p. 467-607.
4. Robertson, B. "Effect of arbitrary temperature and flow profiles on the speed of sound in a pipe," J. Acoust. Soc. Am., Vol. 62, No. 4, October 1977, p. 813.
5. Robertson, B., and Potzick, J., "A long-wave acoustical technique for measuring gas flow in a tube," in preparation.
6. Streeter, Victor L., "Fluid Properties," Handbook in Fluid Dynamics, McGraw-Hill Book Co., Inc., New York, N.Y., 1961.
7. Ref. 3, "Acoustic Wave Motion," pp. 227-305.
8. Wexler, Arnold, and Hyland, Richard W., "Formulations for the Thermodynamic Properties of Dry Air from 173.15 to 473.15K, and of Saturated Moist Air from 173.15 to 372.15K, at Pressures to 5 MPa," May 1980, as yet unpublished.
9. Potzick, J., and Robertson, B., "Synchronous marker for measuring phase in the presence of noise," Rev. Sci. Instrum., Vol. 48, 1977, p. 1290-1294.
10. Potzick, J., and Robertson, B., "Voltage-controlled phase shifter for measuring transfer function in the presence of noise," Rev. Sci. Instrum., Vol. 52, 1981. p. 280.

Acknowledgement

This work is supported by the Office of Industrial Programs, Conservation & Renewable Energy, U. S. Dept-of-Energy, Mr. Stanley F. Sobczynski, Program Manager, under Interagency Agreement #EA-77-A-01-6010.

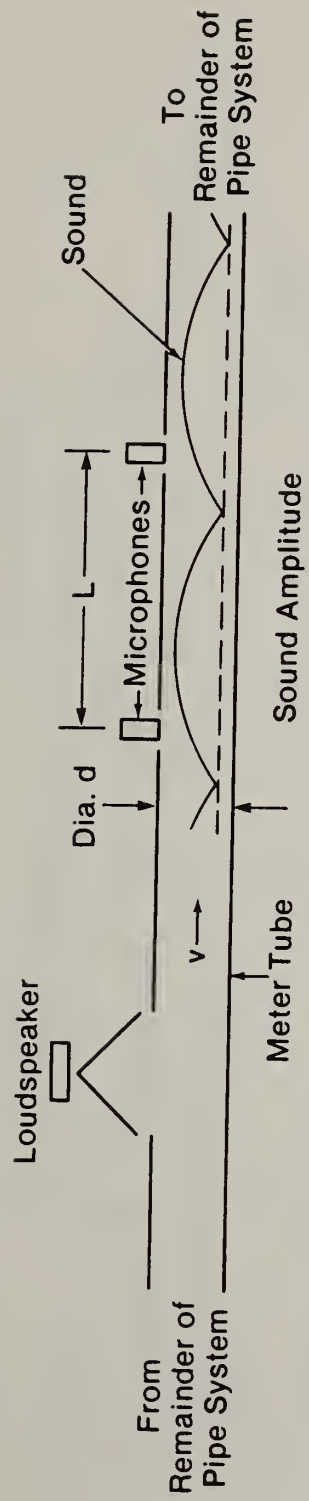


Figure 1. Schematic Diagram of Flowmeter and a Graph of Sound Amplitude vs. Longitudinal Distance

	General Formula	Relevant parameter of prototype meter	Constants used for prototype meter
<u>All Fluids</u>			
Wavelength	$\lambda_n = \frac{2L}{n}$	$\lambda_1 = 0.61 \text{ m}$	$L = 12 \text{ in}$ $= .305 \text{ m}$
Sound speed	$c = 2f_1 L$	$c = 346.3 \text{ m/s at } 25^\circ\text{C}$	$d = 2 \text{ in}$ $= 0.0508 \text{ m}$
Phase difference	$\Delta\phi_n = \omega_n \Delta t = n\pi M$	$\Delta\phi_{1FS} = 18^\circ \text{ for } M_{FS} = 0.1$	$A = 2.027 \times 10^{-3} \text{ m}^2$
Fluid velocity	$v = 2Lf_1 \Delta\phi_1 / \pi$	$\frac{\Delta\phi_1}{v} = \frac{\pi}{c} = 0.520 \text{ deg/(m/s) at } 25^\circ\text{C}$	$P = 1 \text{ atm}$ $= 101325 \text{ Pa}$
Volume flowrate	$Q = 2LAf_1 \Delta\phi_1 / \pi$	$\frac{\Delta\phi_1}{Q} = 0.252 \text{ deg/(l/s) at } 25^\circ\text{C}$	$\gamma = 1.40 \text{ for air}$ $Z = 1.00$
<u>Gases</u>			
Temperature	$T = \frac{m}{\gamma R} 4f_1^2 L^2$	$T = 0^\circ\text{C}$ 25°C 200°C	
Density	$\rho = \frac{\gamma P}{4L^2 f_1^2}$	$f_1 = 543.4 \text{ Hz}$ 567.7 Hz 715.1 Hz	
Mass flowrate	$G = \frac{\gamma PA}{2\pi f_1 L} \Delta\phi_n$	$\frac{\partial f_1}{\partial \rho} = -237.15 \text{ Hz/(kg/m}^3) \text{ at } 25^\circ\text{C}$	
Mass flowrate	$G = \frac{\gamma PA}{L} \Delta t$	$\frac{\Delta t}{G} = \frac{L}{\gamma PA} = 1.06 \text{ } \mu\text{s/(g/s)}$	

Figure 2. Summary of Acoustic Flowmeter Operating Characteristics

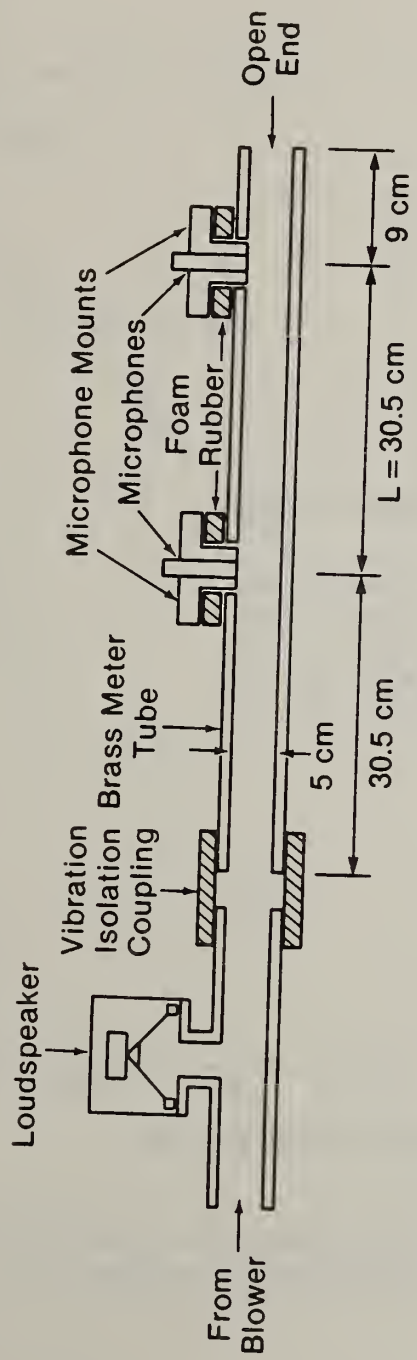


Figure 3. Prototype Acoustic Flowmeter

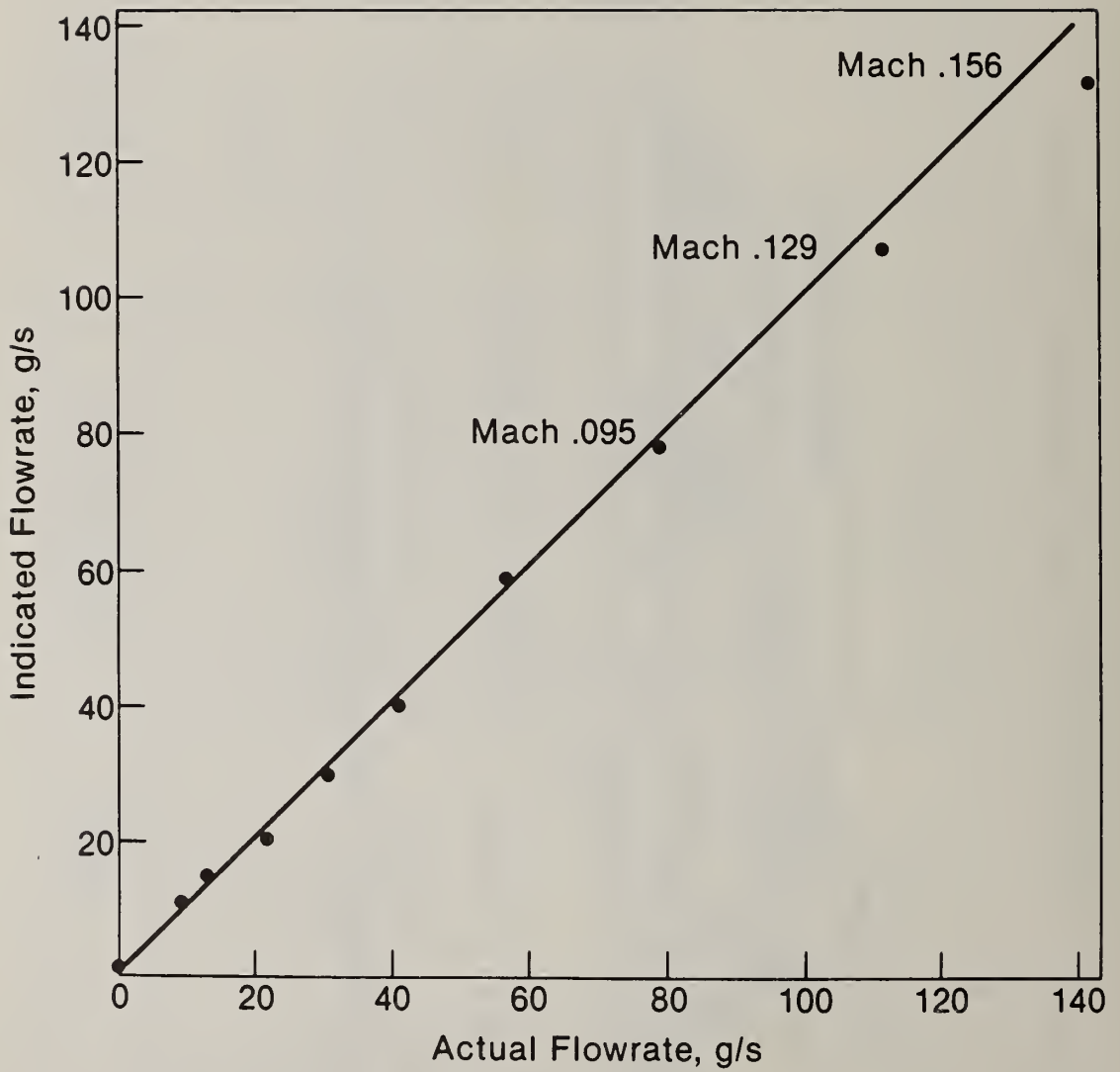


Figure 4. Calibration of analog version of acoustic flowmeter. The line is fit of all data below Mach 0.1

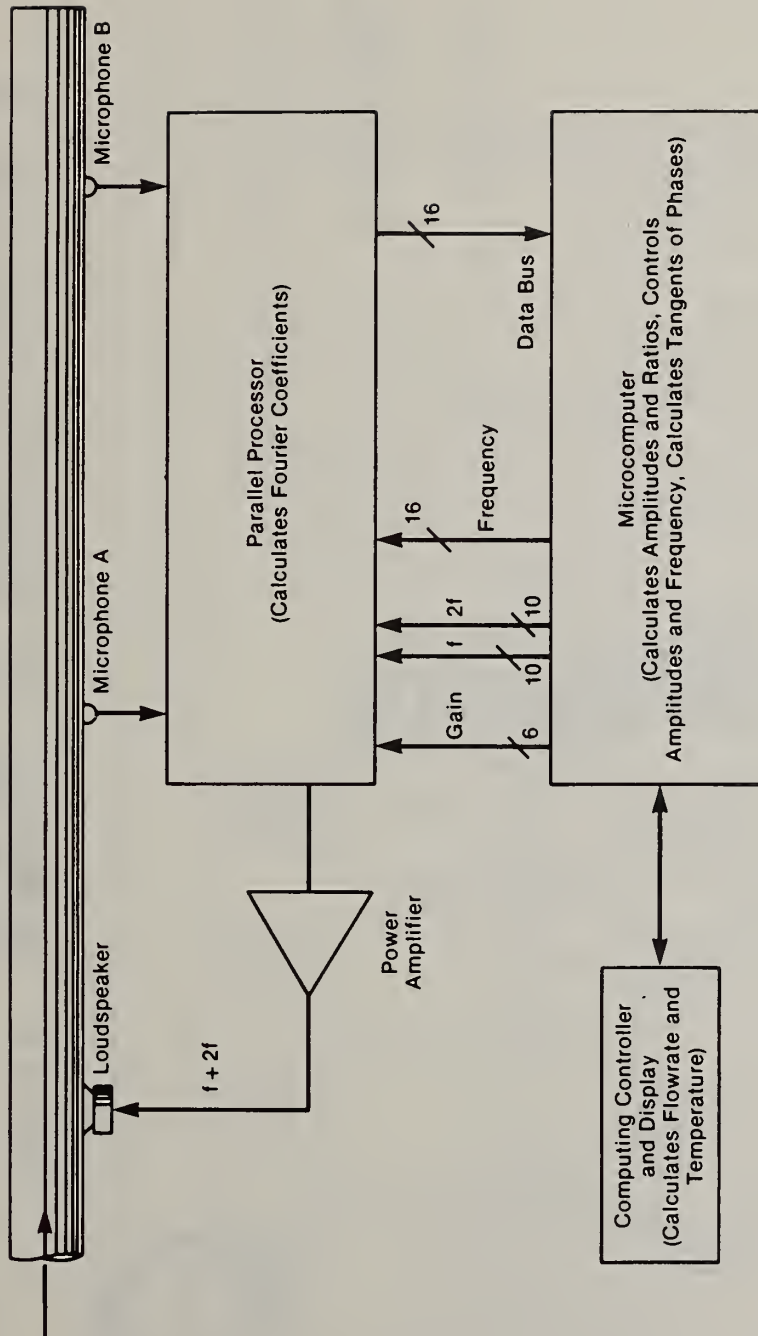


Figure 5. Block Diagram of Acoustic Flowmeter

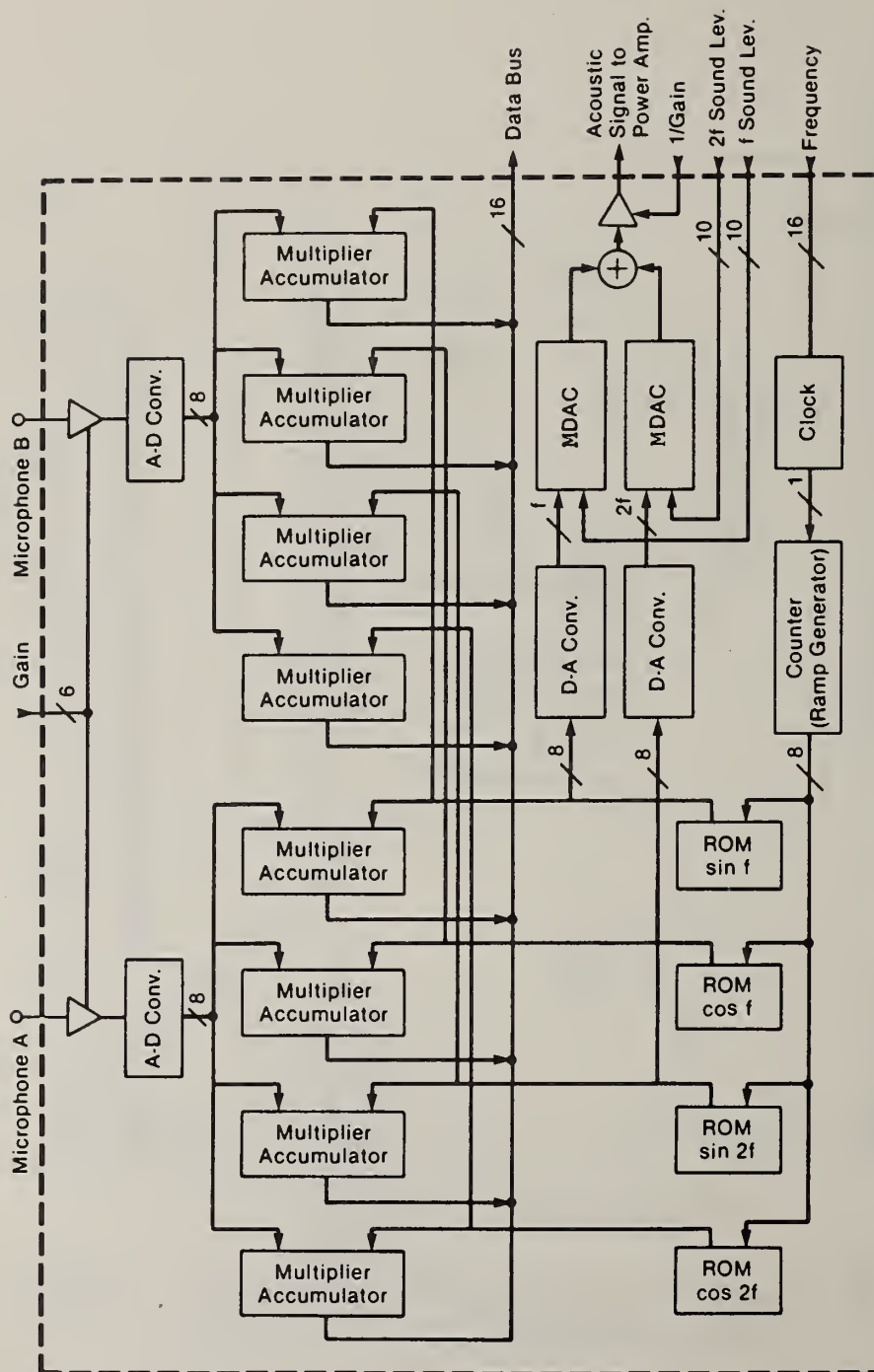


Figure 6. Block Diagram of Parallel Processor

ISA PREPRINT

C.I. 82 — 928

**EVALUATION OF O₂ AND CO MONITORING SYSTEMS
FOR COMBUSTION CONTROLS**

C. Presser, H. G. Semerjian, M. Juberta

ISA/IBP

**International Conference and Exhibit
Philadelphia, Pennsylvania
October 18-21, 1982**



INSTRUMENT SOCIETY OF AMERICA

67 Alexander Drive

P.O. Box 12277

Research Triangle Park

N.C. 27709

U.S.A.

EVALUATION OF O₂ AND CO MONITORING SYSTEMS
FOR COMBUSTION CONTROLS

C. Presser, H.G. Semerjian and M. Juberts

Thermal Processes Division
Center for Chemical Engineering
National Engineering Laboratory
National Bureau of Standards
Washington, D.C. 20234

ABSTRACT

A study has been carried out to provide an evaluation of CO and O₂ monitors used for combustion controls, and to provide reliable data on their performance, operating range and accuracy. The experiments have been carried out in the NBS experimental furnace, which is equipped with a complete on-line gas analysis system used as a reference system. Specific areas of interest included evaluation of the accuracy and sensitivity of the measurement techniques over a wide range of operating conditions, correlation of flame stoichiometry with stack measurements, and the effect of stack gas temperature on composition measurements. The O₂ stack gas monitor has a ZrO₂ type sensor. The system was found to be very sensitive to air leakage when the furnace pressure was kept below atmospheric. A calibration system was also found to be necessary, especially for aspirating type probes. The CO monitoring system is based on infrared absorption across the stack. The CO measurements were found to be quite sensitive to stack gas temperatures, and this effect has been quantified in a heated test cell. The relationship between the stack gas CO levels and combustion zone stoichiometry was also found to be sensitive to the energy extraction rate in the furnace cavity. Experimental results are presented for both natural gas and No. 2 oil fired systems.

I. INTRODUCTION

Industrial efforts to improve the efficiency of boilers and furnaces have led to the development of a number of automatic control systems, which regulate the fuel and air flow rates and try to optimize combustion and energy transfer processes [1]. The approach used for combustion control is to monitor the level of CO and/or excess O₂ in the flue gases. For typical boiler configurations, automatic control is desirable over the concentration range of 100-300 ppmv CO and 0-3% excess O₂ [2-5]. In-situ CO monitors are based on the measurement of infrared absorption across the stack gases [6]. Excess O₂ is determined by the electrochemical reaction occurring across a test-tube shaped zirconium oxide (ZrO₂) probe [7-9].

The installation of these analyzers in the stack may present problems since stack conditions may not be representative of conditions inside the combustion chamber. Air infiltration can significantly influence the O₂ concentration, and to a lesser degree the CO level [10]. The relative advantages of using CO and O₂ monitoring systems, or both, for combustion control have been debated in the literature [11-14]. Several studies have identified automatic on-line control of combustion processes as a generic technology, which can provide energy savings and an improvement in process efficiency for a wide variety of industries [15-19].

This study evaluates an in-situ CO and an O₂ monitor, in the NBS experimental furnace, which is equipped with a complete on-line gas analysis system. Specific areas of interest were evaluation of the accuracy and sensitivity of the measurement techniques over a wide range of operating conditions; effect of higher inlet temperatures (for installations with heat recovery systems) on the stack gas composition; effect of furnace cavity (or stack) pressure level on the CO and O₂ measurements; and the effect of variations in the stack gas temperature.

II. DESCRIPTION OF THE EXPERIMENTAL SETUP

a) Experimental Furnace

The experimental furnace (Figure 1) has a combustion chamber, with the internal dimensions of 80 cm (W) x 110 cm (H) x 240 cm (L). A single burner fires horizontally through one end into the combustion chamber. The combustion products exhaust from the opposite end of the chamber, past a recuperator, and then up through the stack. The furnace has a rated capacity of 300 kW (1×10^6 BTU/hr). Several ports are located along both furnace side walls and the downstream end wall (Figure 1). These ports permit visual observation of the flame, the introduction of intrusive probes and provides an optical path across the furnace. The burner [20] is designed to recirculate and entrain combustion products with incoming fresh combustion air, preheated up to 900°C, thereby enhancing flame stability. Either natural gas or No. 2 fuel oil can be supplied to the burner. Atomizing compressed air is mixed with the liquid fuel, externally, immediately downstream of the nozzle head. Cooling air is passed around the fuel injector in order to reduce thermal decomposition of the fuel. A refractory stabilizer plate provides a separation between the preheated combustion air and the fuel supply line. The recuperator is designed to preheat incoming combustion air to 1550°C before reaching the burner. A high temperature damper located inside the stack is used to maintain positive furnace pressure during experiments. A 4 kW (5Hp) turbo blower supplies combustion air to the burner, having a rated maximum capacity of 23,100 l/min (49,100 ft³/hr). A variable thermal load heat exchanger consisting of two water-cooled 25.4 cm (10 in) diameter stainless steel tubes is used to remove 30-50% of the furnace thermal energy.

b) Gas Sampling and Analysis System

A complete on-line gas analysis system is used for combustion gas sampling and analysis (Figure 2). A water-cooled sampling probe supplies sample gas to a heated bellows vacuum pump through a 460 cm (15 ft) section of heated line. The gas sample is then delivered through a 1070 cm (35 ft) section of heated line to the analyzer manifold. The heated lines and the pump are preheated to 150°C. Gas sample is delivered to the analyzers, entering first a FID type total hydrocarbon analyzer which provides a wet reading. The manifold then leads into a gas dryer which removes water vapor in the sample by permeation distillation. The resulting dry gas is then introduced into the following detectors; Beckman* CO, CO₂ and O₂ analyzers, and TECO NO/NO_x and SO₂ analyzers. Unused sample gas is bypassed into the sample dump manifold. All analyzers are checked and calibrated prior to start of and during a test sequence.

c) Data Acquisition System (DAS)

A Digital Equipment Corp. (DEC) PDP 11/60 minicomputer based data acquisition and control system is used to monitor and record the many instrument variables involved in operating the furnace. Since the computer facility is located 610 m (2000 ft) away from the furnace, a Remote Industrial Control (ICR) I/O subsystem is used to interface the process instrumentation and control signals to the minicomputer. The following list presents those furnace input parameters which are converted and entered into the computer mass storage: coolant water flow, air flow, natural gas and oil flows and stack emissions by the gas sampling system (CO, CO₂, HC, NO, O₂, SO₂, NO/NO_x). A Fluke data logger is used to process and record the various furnace temperatures, being compatible with T, K, R and S type thermocouples. The data logger has a data acquisition rate of approximately 13-15 channels/sec. A Kennedy 75 ips, 9 track, 800 or 1600 bpi magnetic tape transport system is used for storing raw and processed data on tape. A Versatec high speed printer/plotter is used for hard copy listings and for plotting.

d) In-situ Oxygen Analyzer

An in-situ O₂ monitor with an yttria stabilized zirconia tube probe (Figure 3) was located at the far end wall of the furnace. The probe consists of zirconium oxide (ZrO₂) high temperature solid electrolyte ceramic material shaped like a test tube. Two porous platinum electrodes coat the inside and outside surfaces of the zirconia substrate and conduct electricity by means of oxygen ion transport across the cell. The sensor temperature is set at 700°C in order to ensure good ion conduction (voltage output) across the cell. The high temperature also serves to keep the flue gas hot and to burn away any

*Certain commercial equipment, instruments or materials are identified in this report in order to adequately specify the experimental procedure. In no case does such identification imply recommendation or endorsement by the National Bureau of Standards, nor does it imply that the material or equipment is necessarily the best available for the purpose.

combustible material. The sensor probe uses an aspirating extraction technique to transport the sample gas from the probe inlet to the sensing cell. The monitor is calibrated by matching the O_2 concentration with atmospheric air (i.e., 20.9% O_2).

e) In-situ Carbon Monoxide Analyzer

The in-situ CO monitor (Figure 4) is an infrared device that uses a high resolution absorption spectroscopy technique to measure CO in the range of 0-1000 ppmv. An IR light source emitting a wide beam of polychromatic light is chopped at a frequency of 63 Hz and collimated before being transmitted through a sapphire window interface and across the furnace stack to a duplicate sapphire window and collecting mirror on the detector side. Blowers protect the sapphire windows from combustion products, soot and high stack temperatures. The detector cell collecting mirror directs the attenuated beam into a wavelength discrimination module which employs a gas cell correlation technique. A narrow band filter (at $4.7\mu m$) located in front of an electronically cooled lead-selenide detector allows only the CO sensitive portion of the infrared spectrum that is not absorbed by the stack emissions to pass. Each signal is amplified and transmitted via a signal cable to the control room module. The instrument calibration is determined by comparing the monitored CO level to a preset check value of 780 ppmv CO which is based on a 91 cm (3 ft) path length. When the signal voltage drops below 1V the opacity in the stack is 80% or greater and insufficient light is being transmitted across the stack.

III. RESULTS

The experiments were designed so that the concentrations recorded by the O_2 and CO in-situ monitors could be compared with those measured with the gas sampling system. The gas sampling/analysis system has a much slower response and is inadequate for control purposes; however, it provides accurate and reliable measurements. Experiments were conducted with both natural gas and No. 2 fuel oil. The fuel/air equivalence ratio ϕ was varied from about 0.75 to 1.05, the region around $\phi=1.0$ being the main area of interest.

a) Measurements Below the Recuperator

For the first set of experiments, both the O_2 and CO in-situ monitoring systems were located in the region below the recuperator. The in-situ CO monitor was located at the same height with the O_2 probe. The stack gas sampling probe was inserted into the stack through a port which enabled gases to be sampled from the area immediately above the region where the infrared beam traverses the stack cavity. The furnace pressure was kept positive, thereby preventing air infiltration into the furnace. The furnace was preheated for 3-4 hours (to about $900^\circ C$) before data acquisition was initiated. Included are results obtained with the gas sampling/analysis system, with the in-situ O_2 monitor, and from equilibrium calculations based on stack temperature measurements. It should be pointed out that the CO_2 , O_2 and CO measurements obtained from the gas analysis system are "dry" measurements. These readings are then corrected using a flue gas concentration carbon balance and are then reported as the "wet" values. These are, of course, the appropriate values for comparison with the in-situ measurements and the equilibrium calculations.

Typical results for No. 2 fuel oil are shown in Figure 5. The general trends show that as the fuel/air mixture becomes richer (i.e. as ϕ increases) and approaches a stoichiometric mixture, the maximum theoretical value of CO_2 concentration (Figure 5A) is attained (9.5% for natural gas and 15.3% for No. 2 oil) at approximately $\phi=1$, and then starts decreasing beyond that point due to lack of available oxygen. The excess O_2 (Figure 5B) falls steadily, with increasing ϕ , until the stoichiometric mixture is reached, beyond which point no more oxygen is detected. The CO concentration (Figure 5C) remains below 20 ppmv for fuel lean mixtures, and rapidly rises beyond $\phi=1$. The equilibrium calculations are included in each case, and the general trends agree with the measurements. Experimental data obtained in the furnace over the range $0.95 < \phi < 1.04$ is expanded and shown in Figure 6 for No. 2 oil. Upon closer examination of Figure 6 it can be seen that the CO and excess O_2 curves intersect outside the limits proposed by Gilbert [5] (i.e., less than 100 ppmv CO and 0.1% O_2). These results tend to indicate that, under certain circumstances, the relationship between the conditions existing in the combustion zone and those monitored in the stack could be altered drastically. They also suggest that the range of the control parameters (i.e., CO and O_2 concentration) to be utilized may strongly depend on the particular combustion system configuration and heat extraction profile.

The O_2 measurements obtained with the ZrO_2 probe are also shown in Figure 5B. For the fuel lean flames, these readings are observed to deviate from the gas sampling measurements by more than 0.5% O_2 . Part of this discrepancy is attributed to a lack of a calibration procedure, except at ambient conditions. It was also realized that the

readings could be affected by varying the aspiration flow rate. A second set of measurements made after calibration of the O₂ monitor are also shown in Figure 5B (solid symbols). The difference between the two sets of measurements is indicative of the uncertainty present in the oxygen measurements using this particular ZrO₂ sensor.

Measurements with the in-situ CO monitoring system were also attempted at this location below the recuperator, where the gas temperatures are at or above 500°C. This was considered to be representative of typical industrial furnace-type applications. The nominal optical path across the stack was 91 cm (3 ft). This corresponded to the inner wall dimensions, since the cooling air for the sapphire windows also purged the connecting flanges between the external (source or analyzer) units and the furnace inner wall. The blower air flow was assumed to be small enough not to penetrate the central part of the stack, and simply flow up along the walls with a minimum amount of influence on the CO readings. This indeed may be the case for industrial applications, where the in-situ CO monitoring system is usually placed on a boiler stack with a diameter several times that of the experimental furnace, with correspondingly larger flow rates. Unfortunately, because of the smaller size of the NBS furnace, the cooling air was found to penetrate into the stack gases, effecting not only the CO readings, but also the measurements obtained with the ZrO₂ probe and the gas sampling probe. Both of these probes were located near the center of the stack, indicating substantial air penetration. Attempts were made to minimize the cooling air; however, the readings obtained from the in-situ CO monitor were still far lower than those obtained from the gas analysis system. In addition, it was also observed that radiation emitted from the hot furnace walls, especially after several hours of heating, effected the detector signal. This radiant energy, however, is emitted as a continuum and effects only the d.c. level. Therefore, the frequency discrimination capability of the analyzer should compensate for this effect.

Based on these observations, it was concluded that our inability to obtain reliable data at this location was primarily due to the higher stack gas temperatures, which resulted in a reduced absorption coefficient, and hence reduced the indicated CO levels. It was decided to relocate the in-situ CO monitoring system in the stack above the recuperator, where the gas temperatures are substantially lower.

b) Measurements Above the Recuperator

The in-situ CO analyzer was fixed to the tapering portion of the stack above the recuperator (Figure 1). The gas sampling probe drew effluent at a location above the infrared beam so that one could detect dilution effects by the CO monitor cooling blowers. The initial tests produced a large increase in the excess O₂. After restricting the blower output with several pieces of shim stock, it was found that when the opening was too small the monitor output signal voltage would drop until the beam opacity reached beyond 80%. Insufficient air cooling allowed flue gases and soot particles to enter the instrument connecting flanges. The increased path length permitted the CO level to grow rapidly until the analyzer could not continue to operate. The best results obtained are shown in Figure 7, producing a 0.5% increase in the stack excess O₂ and a reduction in the detector electronic signal from 2V to 1-1.5V. It was impossible to produce a full 2V signal without increasing significantly the stack excess O₂. The inability to obtain a strong detector signal without excess O₂ dilution may indicate that the cooling air does not pass through the connecting flanges uniformly, and permits effluents to move into the flanges at the same time. The air may pass into the flanges tangentially and develop a swirling motion with a central recirculating zone which draws flue gases toward the sapphire windows.

The results indicate that the CO₂ peak (Figure 7A) is shifted to slightly larger than $\phi=1$ because of the low furnace temperature (data was recorded at 871°C). The maximum value attained is lower than the theoretical maximum due to the 0.5% excess O₂. The CO level (Figure 7C) will consequently rise when the flame is slightly richer than expected and the excess O₂ (Figure 7B) reaches its minimum past the stoichiometric point. Comparison with the in-situ CO monitor in Figure 7C shows that past stoichiometric conditions both CO readings rise simultaneously, but the in-situ analyzer readings generally remain at less than half the gas sampling value (originally, without the restriction, this ratio was 1:3-4). For automatic control purposes the in-situ instrument could be used as an indicator of the presence of CO, but not necessarily to provide an accurate measurement of the CO concentration. Good agreement between in-situ O₂ monitor and the gas sampling data (Figure 7B) is primarily due to the modified setting of the air aspiration rate.

For stack temperatures below 540°C along with heat removal by the furnace heat exchangers and the recuperator, conditions in the stack may be considered similar to that of a boiler except for the effect of the high temperature flame and furnace wall radiation on

completion of combustion processes. In order to simulate boiler conditions where wall incident energy is negligible data were recorded for lean flames under quasi-steady conditions, Figure 8, during the furnace transient start-up. The results presented in Figure 8 are for $\phi=0.5$ with gas sampling in the stack. The length of each test was approximately 30 minutes which depended upon keeping the stack temperature between 150-190°C. The flame gas temperature rose to 685°C during this trial. Figure 8C shows that there is an initial surge of CO due to poor fuel/air mixing and the cold furnace walls, and then the CO level peaks after several minutes, dropping exponentially as the stack gas temperature increases. During the first 100 seconds the CO₂ concentration (Figure 8A) increases and the O₂ concentration (Figure 8B) decreases rapidly. Afterwards the CO₂ level gradually increases and the excess O₂ drops slowly as the CO level decreases. The CO concentrations recorded from the in-situ device are also shown in Figure 8C. It is again observed that the in-situ CO monitor provides readings which are less than half the value obtained with the gas analysis system, throughout its operating range.

c) In-situ CO Monitor: Investigation of the Effect of Stack Gas Temperatures

It was pointed out earlier that the relatively low CO concentrations measured in the stack gases, with the in-situ CO monitor, were primarily attributed to the higher temperatures encountered in the stack. In order to clearly identify and quantify this effect, an absorption cell was fabricated, where the gas temperature, pressure and composition could be carefully controlled, and CO measurements could be made using the CO monitoring system.

The cell was 91.5 cm (3 ft.) long and was encased by high vacuum flanges. Two sapphire windows, located on the end flanges, allowed optical access into the cell. The sapphire windows were identical to the ones used in the CO monitoring system, so that the spectral response of the system would not be altered. The source and analyzer units of the CO monitoring system were then mounted on the two sides of the cell. A calibration gas mixture of 779 ppm CO/N₂ was introduced into the cell from one end, and the gases exiting from the other end were fed into the gas sampling/analysis system, where the CO concentration was continuously monitored with the nondispersive (NDIR) CO analyzer. The cell was then gradually heated, and the results obtained with both the in-situ monitor and the NDIR analyzer are shown in Figure 9. It can be seen that, while the reading from the NDIR analyzer stayed constant, the measurements obtained with the in-situ monitor decreased by more than two fold as temperature increased from 20°C to 260°C. The results obtained during these experiments document the sensitivity of the in-situ monitor measurements of CO concentration on the stack gas temperature. This dependence on temperature is due to the variation of the absorption coefficient $K = N \cdot Q$, which then affects the infrared light transmission through Beer's Law:

$$T = I/I_0 = \exp(-K \cdot L)$$

where T is the transmittance, I and I₀ are transmitted and incident intensities, respectively, and L the optical path. The absorption coefficient could change either due to changes in the molecular number density N (cm⁻³) or the absorption cross section Q (cm²). The observed reduction in measured absorption, with increasing temperature, could be to a large extent attributed to a decrease in the number density, since the pressure was kept constant. However, this does not account completely for the observed effect, and the remaining change has to be attributed to changes in Q, with temperature, over the spectral bandwidth of the absorption measurements. Results obtained with this simple experiment suggest that accurate measurements of CO concentration in stack gases, using line-of-sight infrared absorption techniques, will require an appropriate correction for changes in the stack gas temperature.

IV. CONCLUSIONS

Performance of two stack gas monitoring systems, a ZrO₂ type O₂ sensor and an in-situ CO monitor based on infrared absorption, has been evaluated in the NBS experimental furnace. Interest was centered around the desired region for automatic controls; viz., 100 < CO < 300 ppm, 0 < O₂ < 2% and 0.95 < ϕ < 1.0.

The in-situ O₂ measurements were found to be quite sensitive to the air aspiration rate, which controlled the gas sampling rate from the stack. The ZrO₂ sensor provides the capability for operating at high temperatures, which is valuable especially for furnace applications. The O₂ sensor, however, was found to be quite sensitive to air infiltration into the furnace from the surroundings, which is quite typical of industrial furnaces and boilers.

Measurements with the in-situ CO monitoring system could be carried out only above the recuperator. Below the recuperator, both the high gas temperature and radiation from the walls appeared to interfere with the measurements. The cooling air proved to cause a substantial amount of dilution effect. In general, the readings obtained with the in-situ CO monitor were less than half of those obtained with the gas sampling system. This deviation was attributed primarily to the effect of gas temperature on the CO absorption coefficient.

It can be concluded that the application of stack monitoring systems for combustion control will require a careful study of the characteristics of the particular installation, before a control system can be implemented which will provide reliable control over the narrow range of operation desired for efficient combustion. These observations also point towards the need for combustion control systems, which do not necessarily rely on stack gas measurements, but rather on measurements made directly in the combustion zone.

ACKNOWLEDGEMENT

Support received from the U.S. Department of Energy, Office of Industrial Programs, under Interagency Agreement No. EA-77-A-01-6010 is gratefully acknowledged.

REFERENCES

1. Robertson, J.L. and Clarke, P.R., "Microprocessors and Instrumentation in Furnace Control," Industrial Heating, Vol. 48, No. 5, May, 1981, pp. 9-12.
2. Gilbert, L.F., "CO Control Heightens Furnace Efficiency," Chemical Engineering, Vol. 87, No. 15, July, 1980, pp. 69-73.
3. Spanbauer, J.P., "Energy Savings Through Advanced Boiler Control," paper presented at the 1980 Annual Meeting of the Technical Association of the Pulp and Paper Industry, 1980.
4. Jutila, J.M., "Guide to Selecting Stack Gas Monitors," Industrial Technology, Vol. 27, No. 11, Nov., 1980, pp. 43-54.
5. Gilbert, L.F., "Precise Combustion-Control Saves Fuel and Power," Chemical Engineering, Vol. 83, No. 13, June, 1976, pp. 145-150.
6. McArthur, L., Lord, H.C. and Gilbert, L.F., "Efficient Combustion Through Boiler Air-Fuel Ratio Control," Final Control Elements, Vol. 3, 3rd Control Valve Symposium and Process Control Technology, Instrument Society of America, Pittsburgh, 1977, pp. 101-106.
7. Hoffman, A.R., "Nature of Platinum-Zirconia Oxygen Sensor," Industrial Heating, Vol. 47, No. 7, July, 1980, pp. 32-33.
8. "Considerations for Energy Savings in Design and Use of Continuous Heat Treating Furnaces - Part I - Role of Controls," Industrial Heating, Vol. 48, No. 6, June, 1981, pp. 33-37.
9. Shafer, R.V., "Oxygen Measurement and Control for More Efficient Operation of Soaking Pits," Industrial Heating, Vol. 48, No. 8, August, 1981, pp. 14-19.
10. Opel, A.E. and Gilbert, L.F., "Closed Loop Source Monitoring Saves Energy and Money," ASME Paper No. 78-WA/APC-6, Dec., 1978.
11. Molloy, R.C., "Microprocessor Based Combustion Monitoring and Control Systems Utilizing In-Situ Opacity, Oxygen, and CO Measurements," presented at the 4th World Energy Engineering Conference in Atlanta, Georgia, Oct. 12-15, 1981 and also presented at the 3rd Annual Industrial Energy Conservation Technology Conference and Exhibition, Houston, Texas, April 26-29, 1981.
12. Richardson, D.M., "Combustion Efficiency through Use of Flue Gas Analyzers," Industrial Heating, Vol. 45, No. 5, May, 1978, pp. 20-21.

13. Anson, D., Clarke, W.H.N., Cunningham, A.T.S. and Todd, P., "Carbon Monoxide as a Combustion Control Parameter," Combustion, Vol. 43, No. 9, March, 1972, pp. 17-20.
14. Pruce, L.M., "Maximum Boiler Efficiency and Save Fuel with CO Monitoring," Power, Vol. 124, No. 1, Jan., 1980, p. 70-72.
15. Hall, E.H. et al, "Evaluation of the Theoretical Potential for Energy Conservation in Seven Basic Industries," Battelle Columbus Laboratory, Report to FEA, January, 1975.
16. Hamm, J.R. et al, "Energy Conversion Alternatives Study (ECAS) - Vol. III: Combustors, Furnaces and Low Btu Gasifiers," Westinghouse Electric Corp. Reserach Laboratories, NASA CR-134941, February, 1976.
17. Resource Planning Associates, "Implementation of Energy Conservation Technology in the Pulp and Paper Industry," Report for Office of Industrial Programs, Dept. of Energy, September, 1980.
18. Fam, S.S., "Impact on Energy Conservation of Automatic Control Systems Utilization in the U.S. Pulp and Paper Industry," Thermo Electron Rpt. No. TE4265-20-80, 1980.
19. "Basic Research in Engineering - Workshop on Fluid Dynamics and Thermal Processes," Engineering Societies Commission on Energy, Inc., February, 1980.
20. Young, S.B., "High Temperature Waste Heat Recovery Systems for Forge and Other Furnaces," Industrial Heating, Vol. 47, No. 7, July, 1980, pp. 16-18.

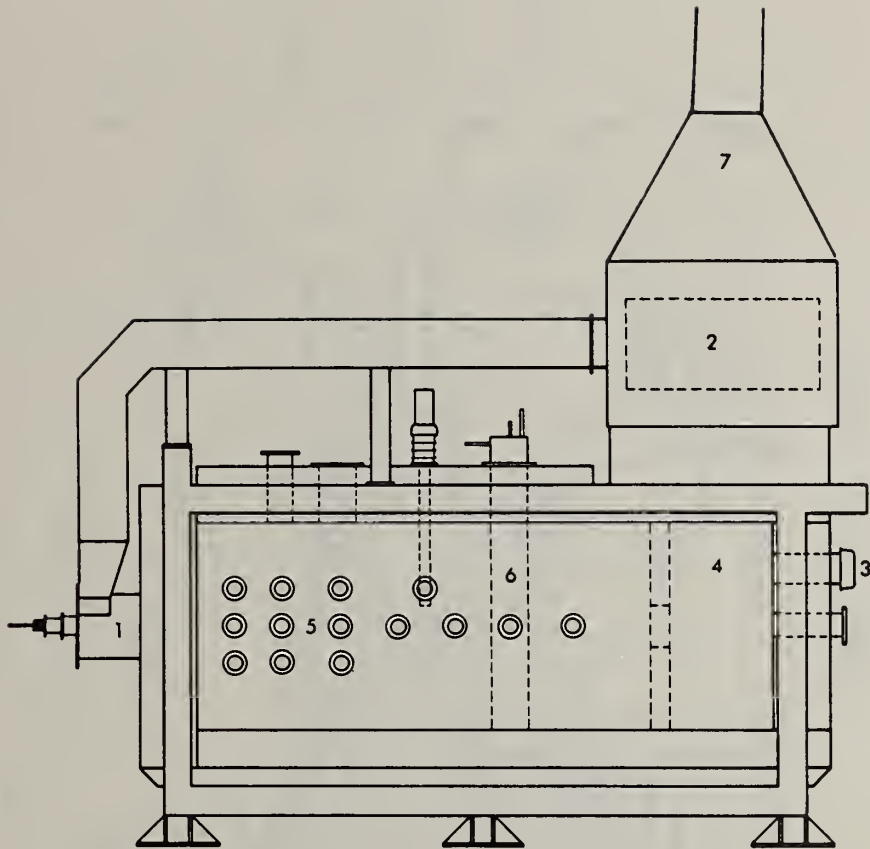


FIGURE 1 - NBS EXPERIMENTAL FURNACE. 1) BURNER; 2) RECUPERATOR; 3) LOCATION OF IN-SITU O₂ MONITOR; 4) LOCATION OF IN-SITU CO MONITOR BELOW RECUPERATOR; 5) PORTHOLES; 6) HEAT EXCHANGER PROBES 7) LOCATION OF IN-SITU CO MONITOR IN THE STACK.

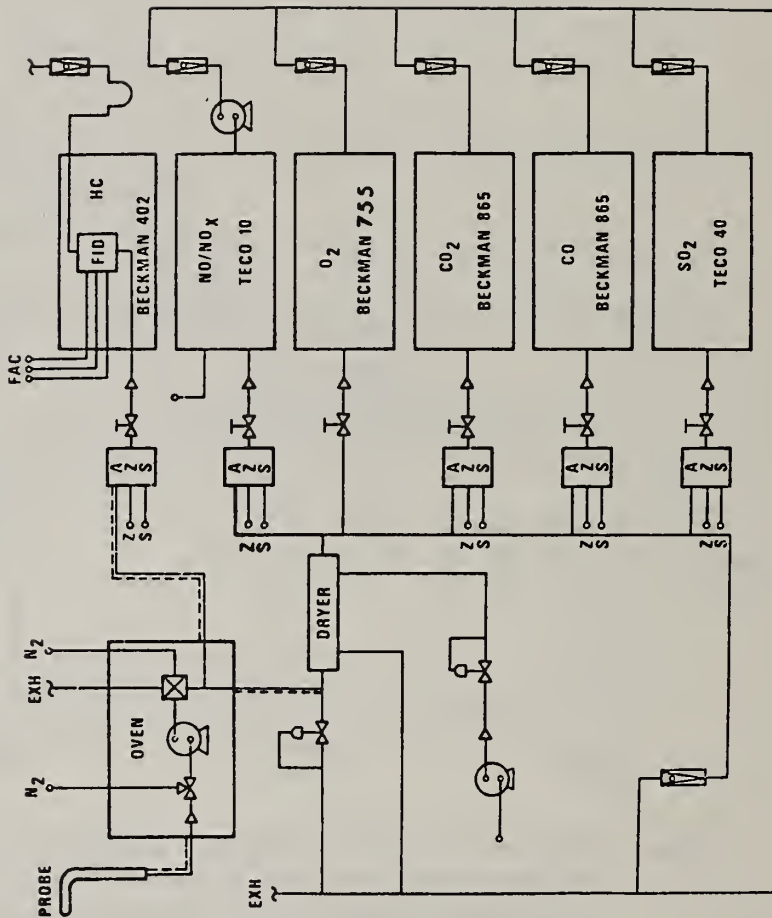


FIGURE 2 - SCHEMATIC OF GAS ANALYSIS AND SAMPLING SYSTEM.

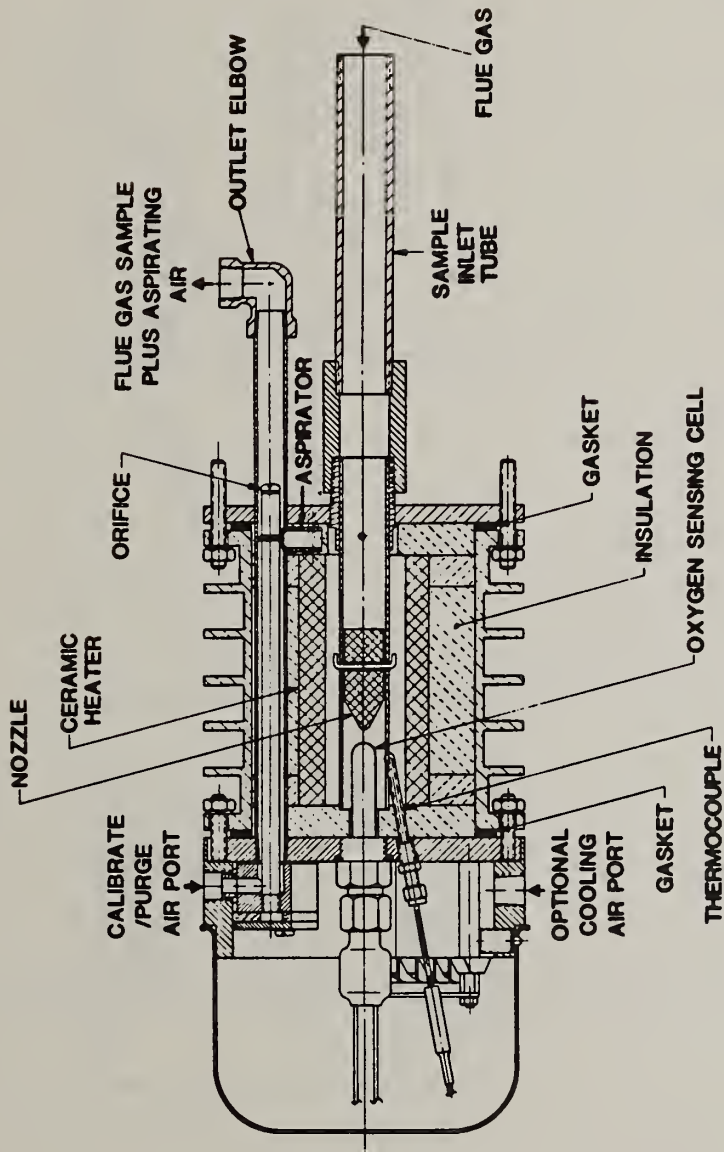


FIGURE 3 - SCHEMATIC OF O₂ PROBE.

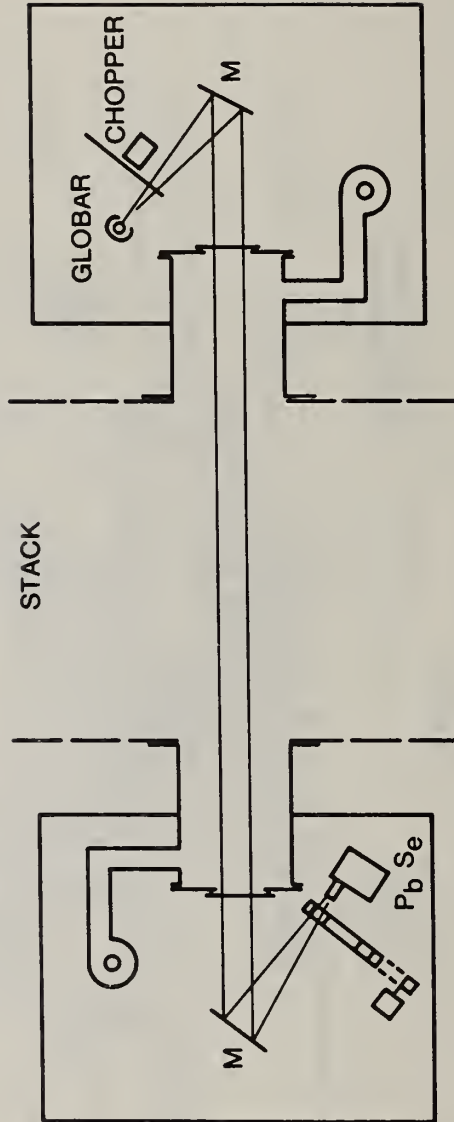


FIGURE 4 - SCHEMATIC OF IN-SITU CO MONITORING SYSTEM.

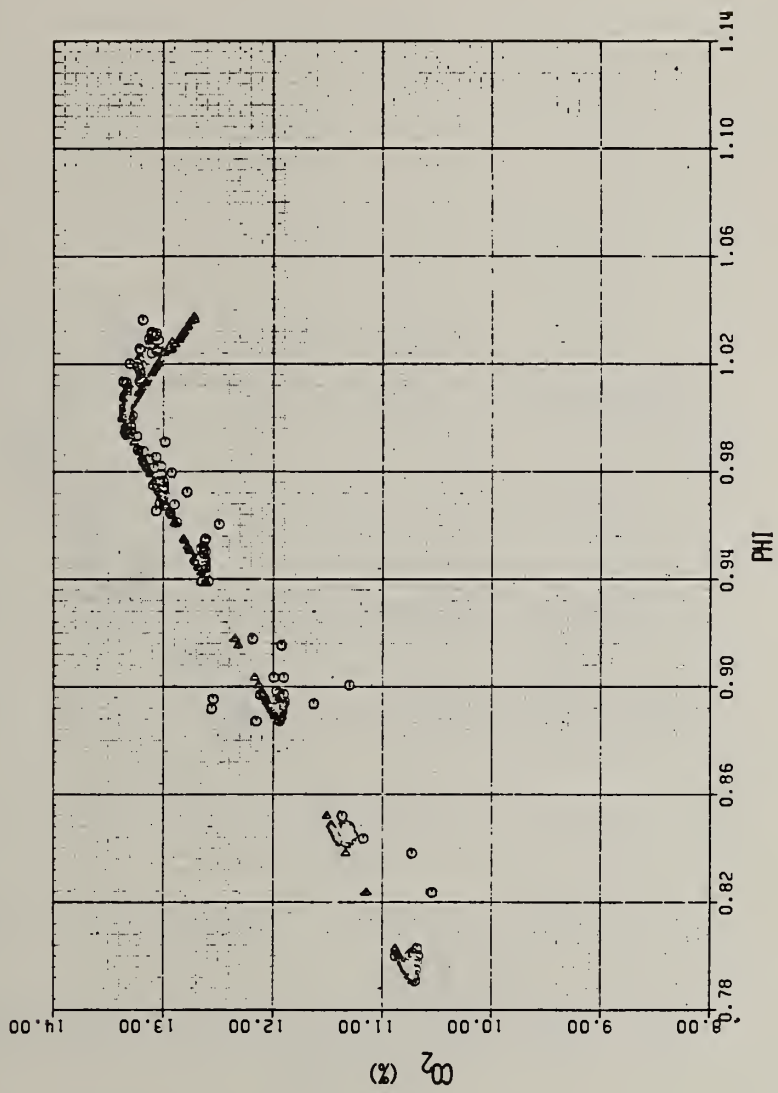


FIGURE 5A - VARIATION OF CO₂ CONCENTRATION WITH EQUIVALENCE RATIO;
No. 2 FUEL OIL; SAMPLING BELOW RECUPERATOR.

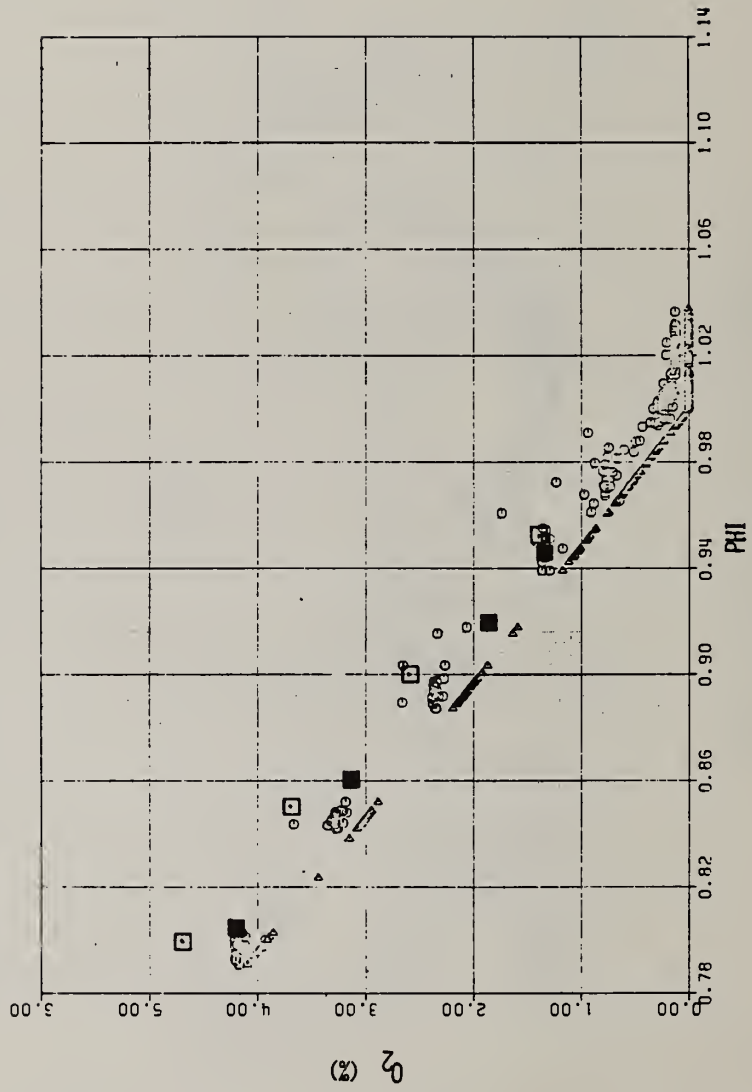


FIGURE 5B - VARIATION OF O₂ CONCENTRATION WITH EQUIVALENCE RATIO;
 No. 2 FUEL OIL; SAMPLING BELOW RECUPERATOR.

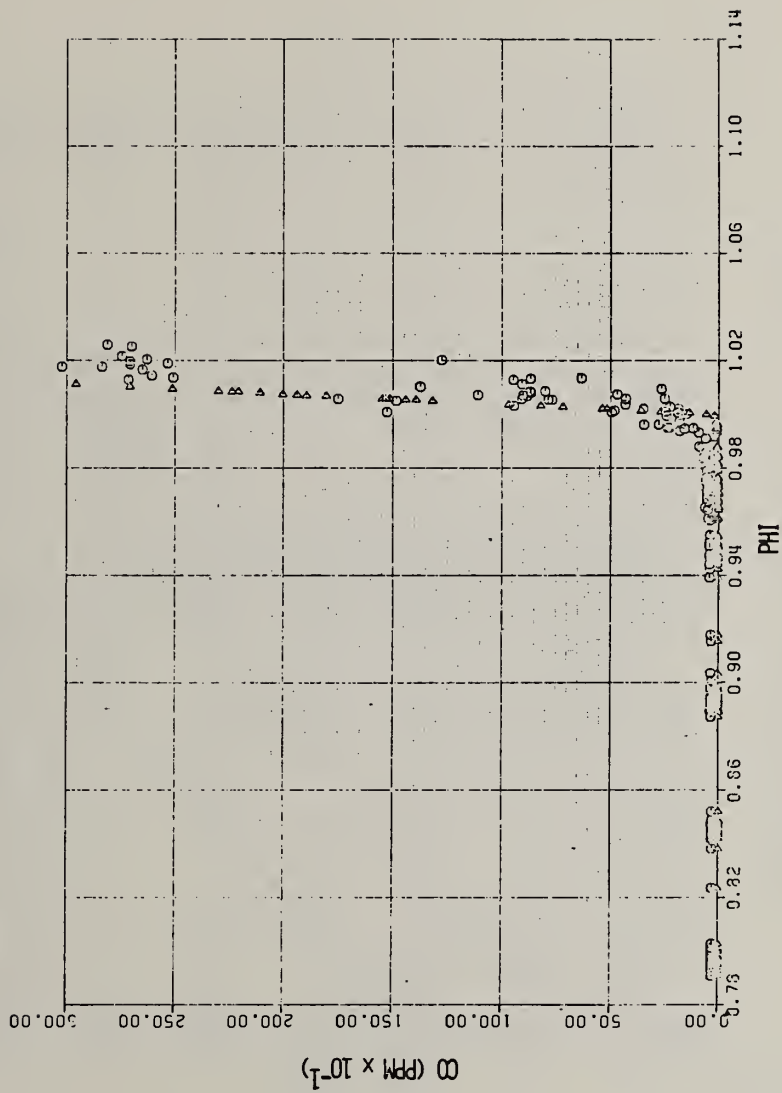


FIGURE 5C - VARIATION OF CO CONCENTRATION WITH EQUIVALENCE RATIO;
No. 2 FUEL OIL; SAMPLING BELOW RECUPERATOR.

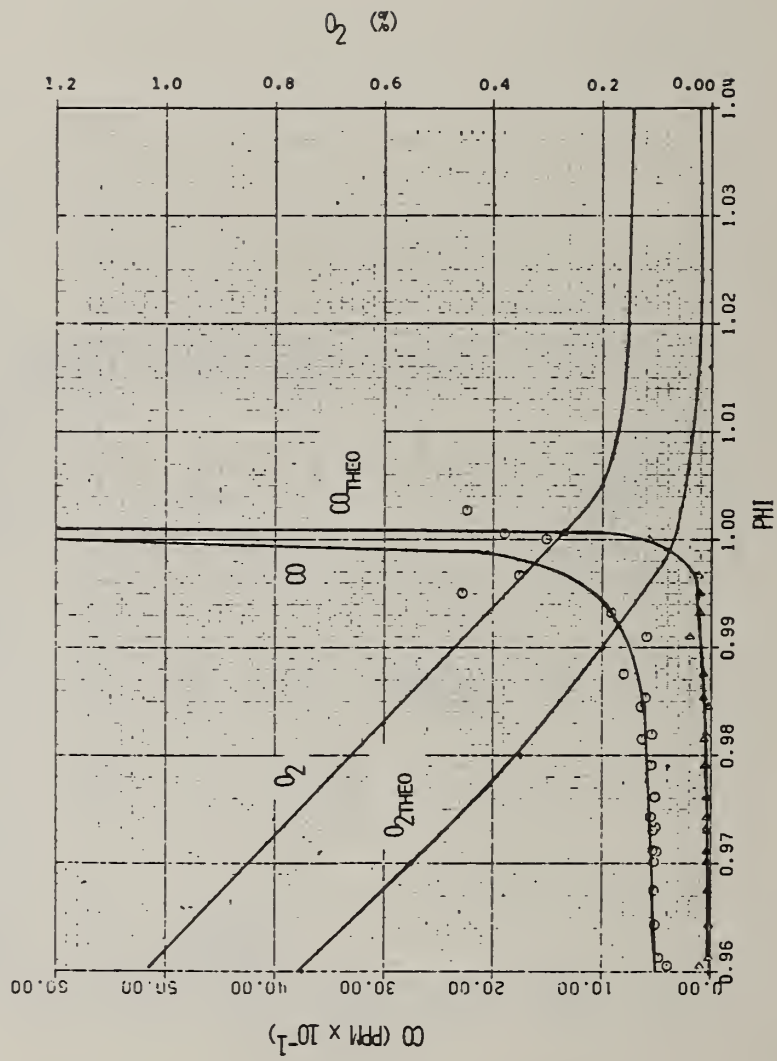


FIGURE 6 - VARIATION OF CO AND O₂ CONCENTRATION WITH EQUIVALENCE RATIO; EXPANDED SCALE; NO.2 FUEL OIL; SAMPLING BELOW RECUPERATOR.

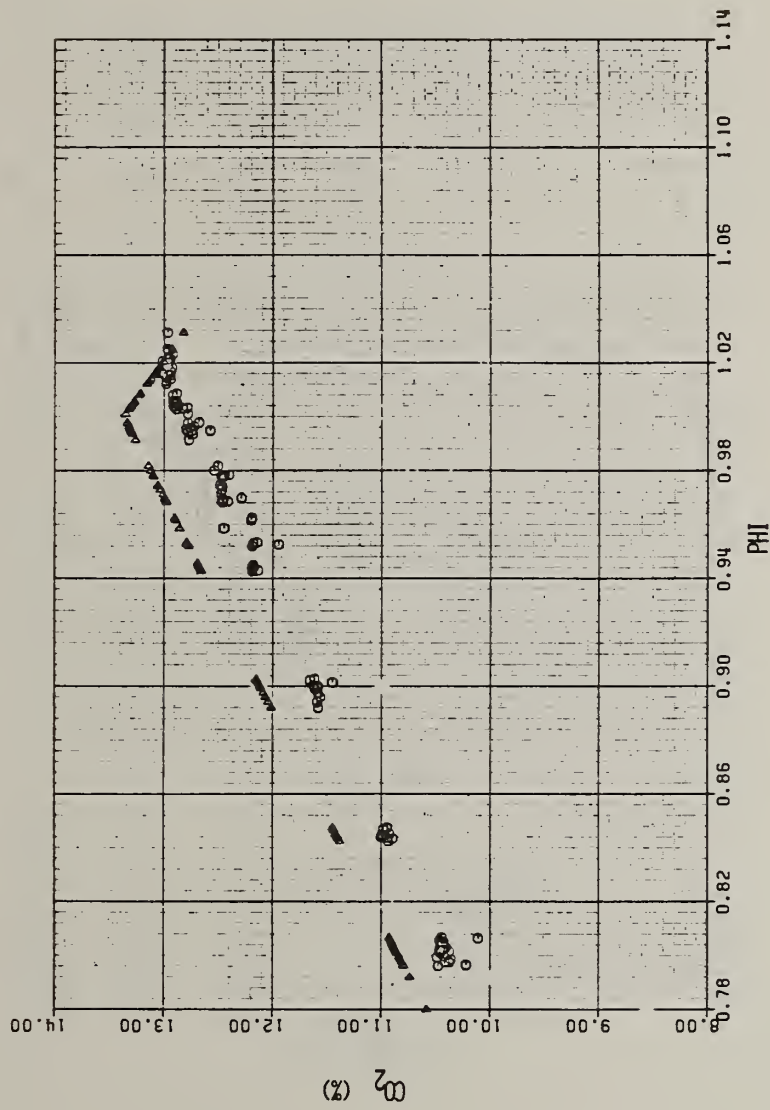


FIGURE 7A - VARIATION OF CO₂ CONCENTRATION WITH EQUIVALENCE RATIO;
 No. 2 FUEL OIL; SAMPLING ABOVE RECUPERATOR.

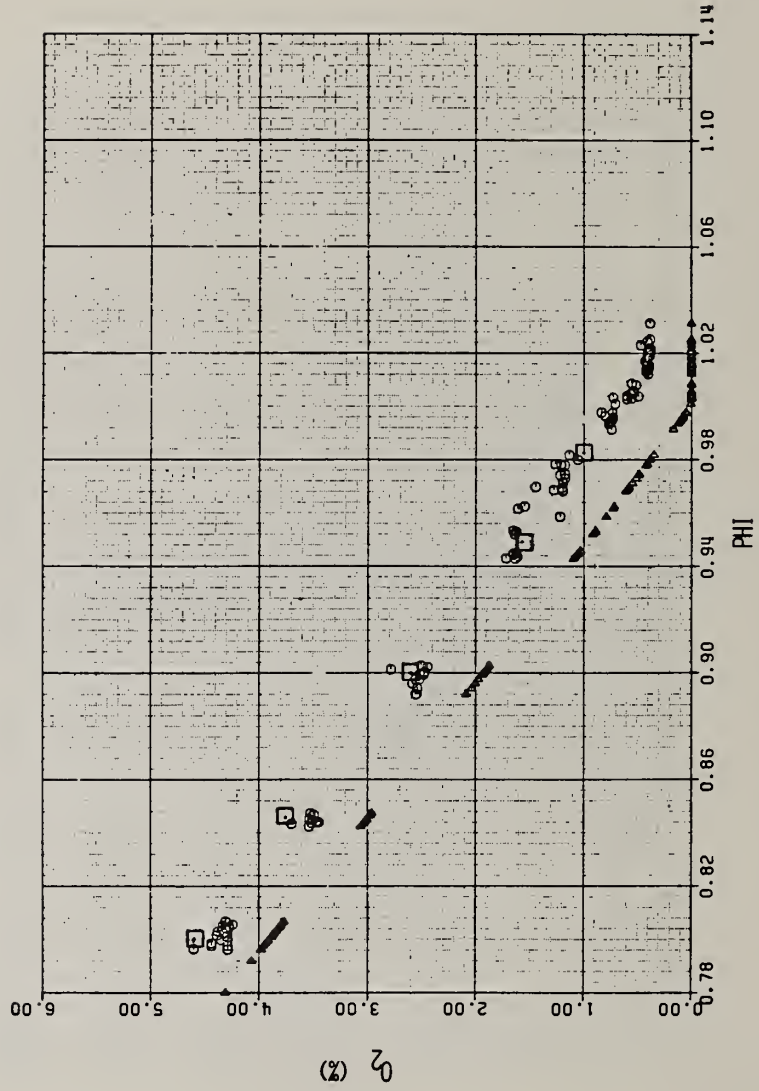


FIGURE 7B - VARIATION OF O₂ CONCENTRATION WITH EQUIVALENCE RATIO;
 No. 2 FUEL OIL; SAMPLING ABOVE RECUPERATOR.

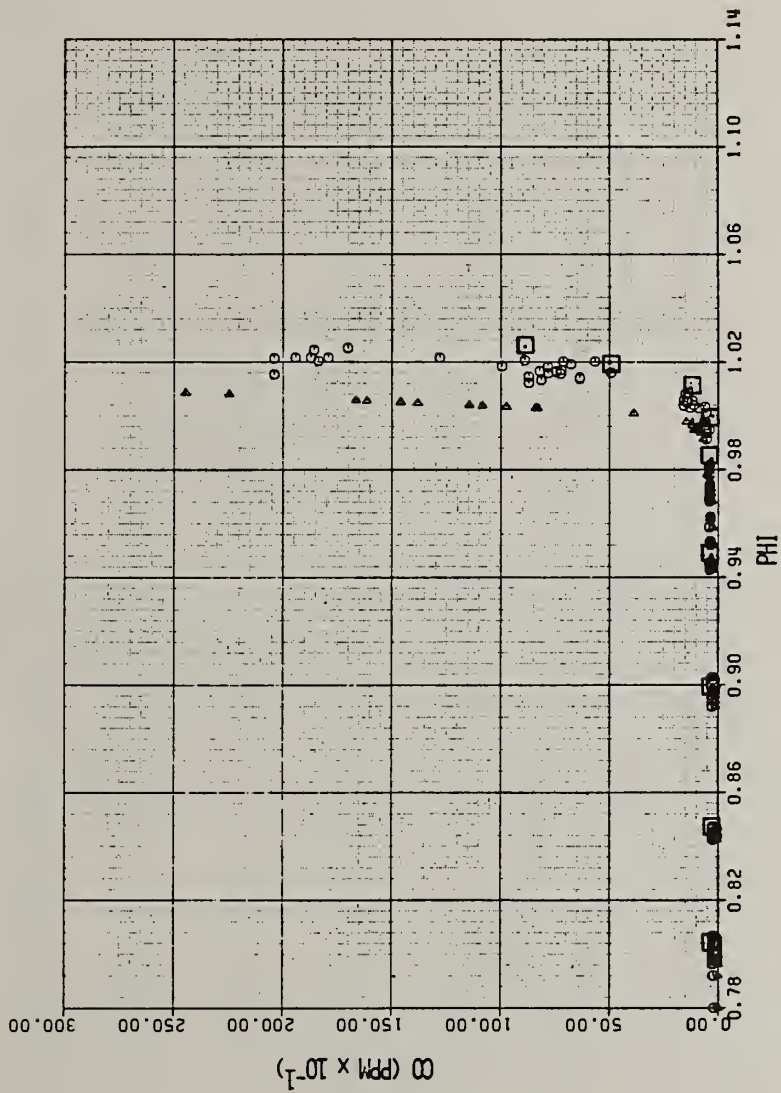


FIGURE 7C - VARIATION OF CO CONCENTRATION WITH EQUIVALENCE RATIO;
 No. 2 FUEL OIL; SAMPLING ABOVE RECUPERATOR.

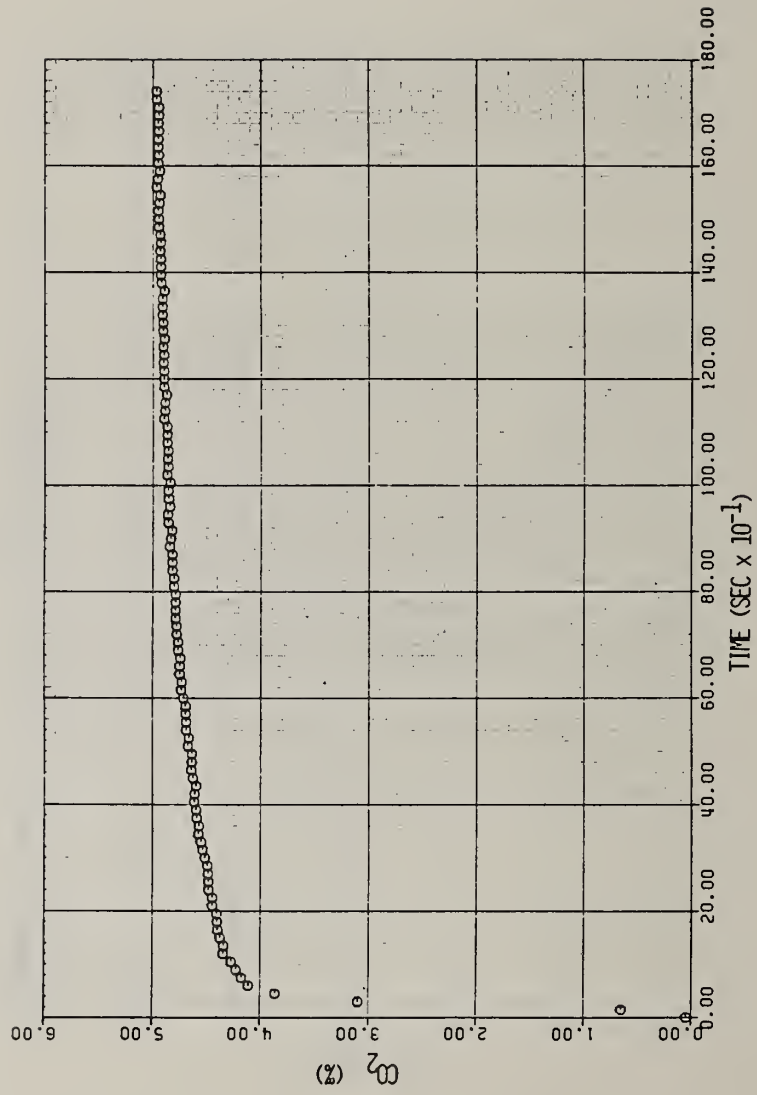


FIGURE 8A - START-UP TRANSIENT TEST: CO₂ VARIATION WITH TIME;
NATURAL GAS; SAMPLING ABOVE RECUPERATOR.

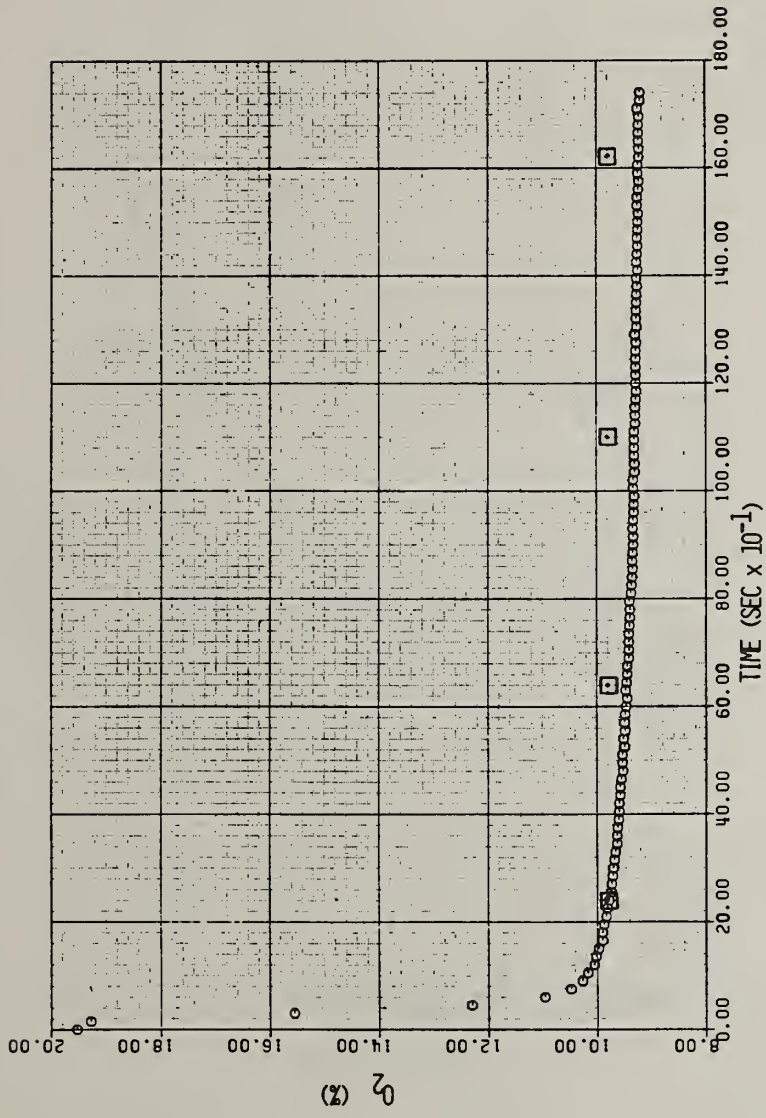


FIGURE 2B - START-UP TRANSIENT TEST: O₂ VARIATION WITH TIME;
NATURAL GAS; SAMPLING ABOVE RECUPERATOR.

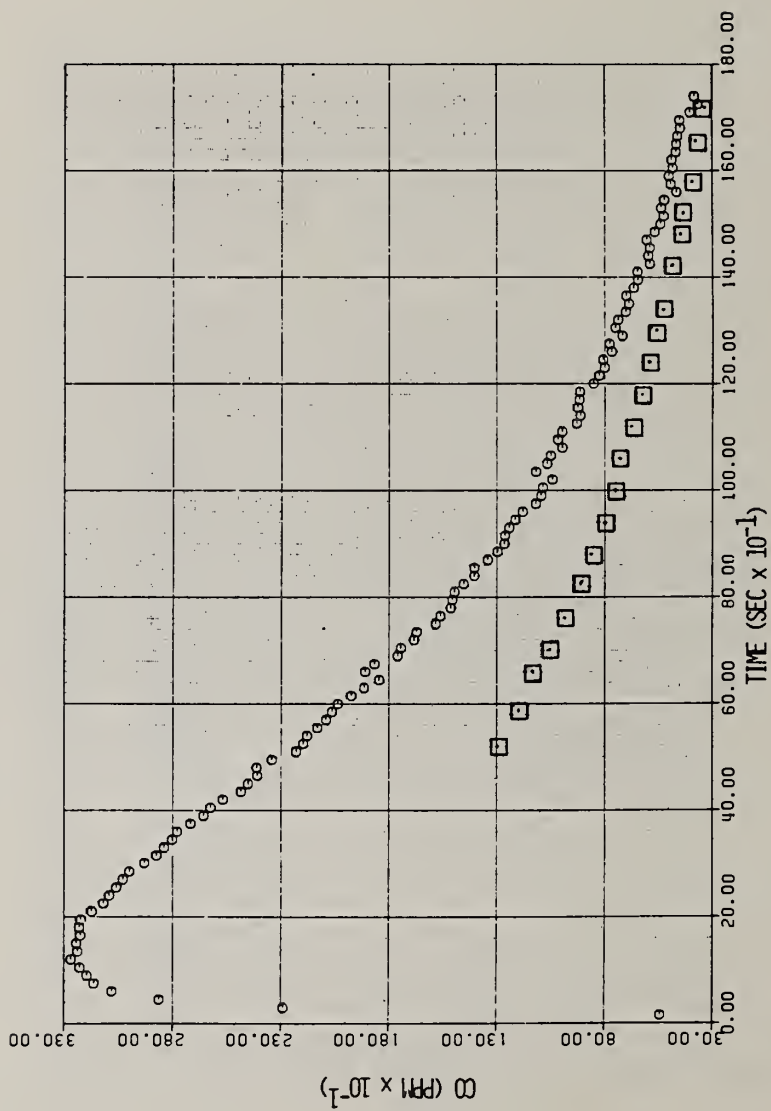


FIGURE 8C - START-UP TRANSIENT TEST: CO VARIATION WITH TIME;
NATURAL GAS; SAMPLING ABOVE RECUPERATOR.

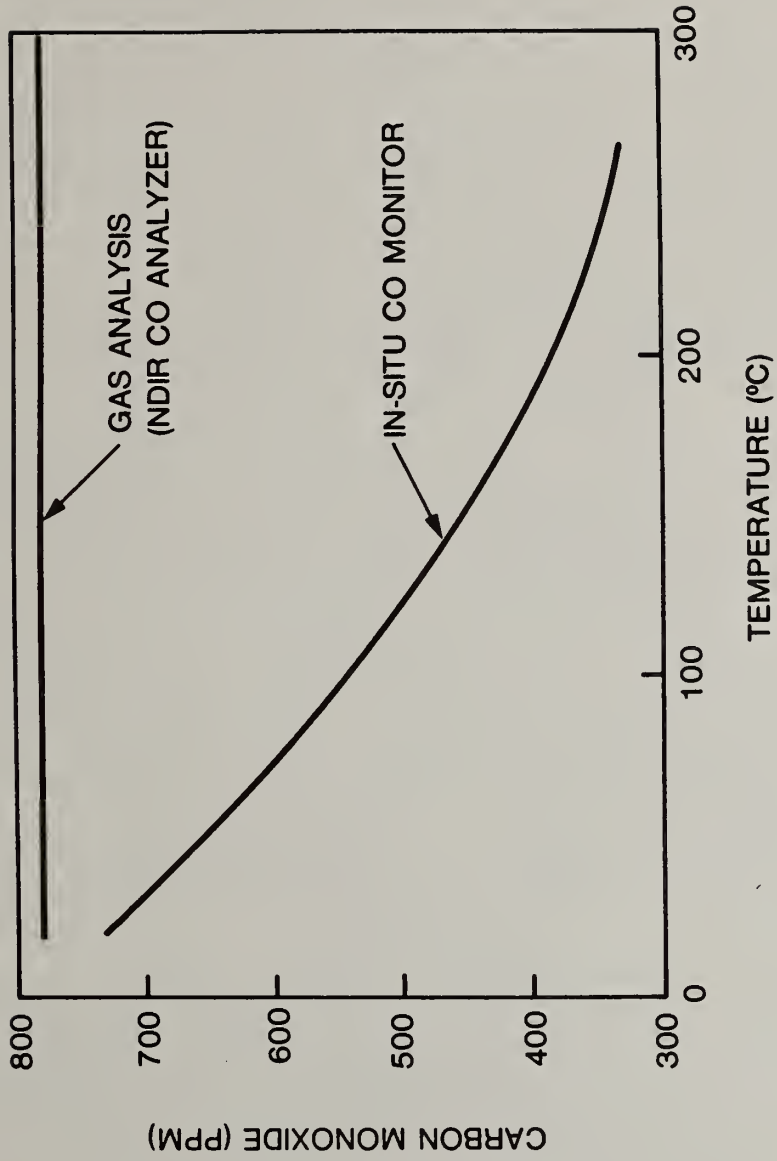


FIGURE 9 - DEPENDENCE OF CO MEASUREMENTS ON TEST CELL TEMPERATURE.

